Chapter 3

Polyethylene/polypropylene/alkali treated-wheat straw-based packaging film

This chapter deals with optimization of alkali-treated wheat straw incorporated polyethylene/polypropylene film using response surface methodology for green packaging application and that was characterized by FTIR analysis, SEM analysis, XRD analysis, WVTR, WVP, contact angle, tensile test, elongation test, impact test, and optical characteristic test.

3.1Introduction

A set of different combination of synthetic polymers such as polyethylene, polystyrene, polyamide, polypropylene, polyethylene terephthalate and polyvinyl chloride are frequently used for packaging application. However, frequent use of non-biodegradable polymers is correlated with the surging plastics wastes. The worldwide production of polymers has grown from 1.5 million tons in 1950 to about 322 million tons in 2015(Bajracharya et al., 2016; Díaz et al., 2018; Dixit and Yadav, 2019; Fazeli et al., 2018). Hence, increasing plastic wastes have affected several environmental aspects. In particular, many environment reports have also proved that polymeric wastes imbalanced the surrounding chains (Law and Thompson, 2014). Therefore, the imbalanced environment triggers disturbance in the lifecycle of many organisms. A dire need for minimizing polymeric wastes provoked many researchers to develop new biodegradable materials as a replacement for synthetic polymers. In addition, many authors have also used abundantly available wheat straw in the polymer matrix for

minimization of polymer wastes and also synthesizing biodegradable polymer with a higher mechanical stability (Bourmaud et al.,2007) .

Some authors have also reported that the polymers blended with pre-treated biomass exhibit a remarkably higher mechanical strength and benchmark thermal stability as compared to native biomass-based composite film (Hou et al., 2014; Laadila et al., 2017).

Many authors used a combination of polyethylene and polypropylene to attain promising melting points, water-resistance and higher resistance to fatigue (Gamage et al., 2009; Jo et al., 2018). However, the non-biodegradability of synthesized composites compelled authors to prepare biodegradable composites using green fiber in a polymer matrix (Mansor et al., 2018; Xie and Hung, 2018). These green fibers are low in density, economical, easily available and provide benchmark mechanical stability to composites. The synthesis of biodegradable packaging film has been encouraged widely, such as the development of a composite involving polymer and abundantly available wheat straw as a packaging matrix. Several authors have reported the suitability of agro-waste blended polymer composites for packaging applications (Ayrilmis et al., 2013; Babaei et al., 2014; Bledzki et al., 2010; Colín-Chávez et al., 2014; Panthapulakkal and Sain, 2015; Pereira et al., 2015; Thakur et al., 2014). Some authors focused on alkali treatment of biomass for increasing the suitability with polymer matrix and enhancing the mechanical stability of composites (da Silva et al., 2013; Hou et al., 2014; Pigatto et al., 2012; Zegaoui et al., 2018). Sometimes Nano-clay and Nano-silver have also been incorporated with polyethylene as a packaging matrix for food preserving application (Ayrilmis et al., 2013; Jiang et al., 2018; Jo et al., 2018; Naskar et al., 2018; Sabetzadeh et al., 2016; Saha et al., 2018; Wu et al., 2017). Authors optimized the mechanical properties of natural rubber incorporated poly (3-

hydroxybutyrate-co-3-hydroxy valerate) matrix for food packaging applications using RSM (Zhao et al., 2019). In this study, glutin/carboxymethyl cellulose/ cellulose nanofiber composite is synthesized and optimized water vapor permeability, colour and mechanical properties of the composite using RSM analysis (Bagheri et al., 2019). Several studies have also provoked to synthesize oxygen scavenging packaging film using a low-density polyethylene matrix (Kim and Holtzapple, 2005; Semanová et al., 2016). This study examined the tensile property of biocomposite synthesized from polylactic acid and treated cellulosic waste (Laadila et al., 2017).

In order to replace the time-consuming conventional methods, RSM is the best choice to optimize the parameters according to the targeted application. RSM is a combination of mathematical and statistical techniques that provide the optimized condition by analysing the relative importance of all affecting factors (Bezerra et al., 2008; Oyekanmi et al., 2019a). RSM is used to observe the simultaneous effects of different independent variables for getting the benchmark output response. Many authors claimed the suitability of using the central composite design of RSM to optimize the independent variables in their research article (Mohamed et al., 2018; Oyekanmi et al., 2019b). RSM is generally a technique to move from initial guess to optimized conditions. It is an empirical model that provides a desirable set of experiments. However, a desirable set of experiments provides response data that is used by RSM to predict the nature of the system (Leardi, 2009). Thus, the primary function of RSM is to optimize the process parameters that maximize the response (Abdulrahman Oyekanmi et al., 2019).

In the current research, polyethylene/polypropylene was blended with alkali treated-wheat straw with the different set of compositions provided by RSM in terms of mass of polyethylene, polypropylene and alkali treated-wheat straw and visualized the effect

on outcome such as tensile strength, elongation at break (%) and water vapor transmission rate. A quadratic model was applied to depict a relationship between mechanical properties and the mass ratio of polymer/biomass. Moreover, various statistical techniques were used to obtain the optimum mass of polymer and biomass with remarkable tensile strength, moderate elongation at break (%) and lowest water vapor transmission rate. The resultant biocomposite film was characterized using XRD, SEM, Mechanical testing, WVTR, contact angle and optical characteristics test.

3.2. Materials and Methods

3.2.1 Materials

Wheat straw, an agricultural waste was collected from a local farm near BHU, Varanasi after harvesting the main product. Initially, wheat straw was washed with distilled water and dried in the presence of sunlight. Wheat straw is ground and sieved through 80 -120 mesh size screens. The wheat straw is passed through 80 mesh screen and retained by 120 mesh screens. So, the average particle size of wheat straw was from 0.177 to 0.125 mm. Polymers such as polyethylene (LR grade) and polypropylene (LR grade) were procured from Sigma Aldrich, USA. Moreover, chemicals such as xylene and sodium hydroxide for alkali treatment were purchased from Fisher Scientific, USA.

3.2.2 Alkali pre-treatment of wheat straw

In this pre-treatment, 5g wheat straw was chemically treated with 1%, 3%, 5%, 7%, 10% of sodium hydroxide at 60˚C for one hour. The desirable residue was filtered and used for reinforcing polymer composites (Nargotra et al., 2018).

$$\textbf{Lignocellulosic biomass –OH} + \textbf{NaOH} \longrightarrow \textbf{(Lignocellulosic biomass- } O^{-}\textbf{)}Na^{+} + \textbf{H}_2\textbf{O} + \textbf{Impurities (1)}$$

3.2.3 Compositional analysis

To study the percentage removal of hemicellulose and lignin from agro-waste, the compositional analysis of agro-waste was performed. Holocellulose, hemicellulose, cellulose and lignin contents of agro-waste and alkali treated-agro-waste were calculated (Bledzki et al., 2010).

3.2.3.1 Lignin contents

To determine the lignin content, 2 g of agro-waste was treated with 15 ml of 72% H_2SO_4 at a temperature of 25^{O}C. The mixture was continuously stirred for two and a half hours. Further, 200 ml of distilled water was mixed in the mixture and heated for the next two hours. After 24 hours, the mixture was washed with distilled water until it attains pH 7. The washed material was dried in an oven at a temperature of 80^{O}C for 8 hours and cooled down in desiccator. The dried lignin material was weighed (Bledzki et al., 2010).

3.2.3.2 Holocellulose contents

For determination of holocellulose, 3 g of dry agro-waste was treated with 0.5 g of glacial acetic acid, 160 ml of distilled water, and 1.5 g of NaCl in a conical flask which was placed in a water bath at a temperature of 75^{O}C for an hour. Subsequently, the same amounts of acetic acid and NaCl were added three times hourly. The resultant solution was placed in an ice bath for 8 hours. The Holocellulose content was separated from the mixture through filtration and washed with acetone, ethanol and distilled water to make acid free material. Holocellulose content was dried in an oven at a temperature of 80^{O}C for 8 hours (Bledzki et al., 2010).

3.2.3.3 Cellulose contents

2 g of holocellulose was treated with 10 ml of 17.5% NaOH at a temperature of 20^{O}C with continuous stirring using a glass rod. Further, 10 ml NaOH was added in the solution repeatedly every 5 min for half an hour. Moreover, 33 ml of distilled water was added to the solution and kept it for another half an hour. The residue was filtered using a filtration unit and washed with 100 ml of 8.3% NaOH and 200 ml of distilled water. After that, the water-washed residue was again washed with 15 ml of 10% acetic acid and 200 ml of distilled water. The washed cellulose was dried and weighed (Bledzki et al., 2010).

3.2.3.4 Hemicellulose contents

The subtraction of cellulose content from holocellulose content gives hemicellulose content present in the agro-waste (Bledzki et al., 2010).

3.2.4 Synthesis of polyethylene/polypropylene/alkali treated-wheat straw

Films with different composition recommended by RSM software were synthesized using solution casting method. A film with different compositions exhibited the total weight of the film. Polyethylene and polypropylene both are non-polar, saturated and high molecular weight hydrocarbons and xylene is aliphatic hydrocarbon. Both simultaneously dissolve in xylene solvent at high temperature. The film was synthesized by dispersing a known amount of polyethylene and polypropylene in xylene at a temperature of 130˚C. The polymeric solution was mechanically stirred at 400 rpm for an hour. Subsequently, native- wheat straw was added in a solution. Then, the solution was mechanically stirred at 600 rpm for half an hour. The bio-composite

solution was cast in a petri dish. Moreover, the cast solution was kept in an oven at 50˚C for 24 hours and the film was detached safely. In a similar manner, the film using alkali treated- wheat straw based polymeric composite was also prepared. In addition, bio-composite films were also preserved using aluminium foil and placed in a desiccator for preventing film from attaining moisture.

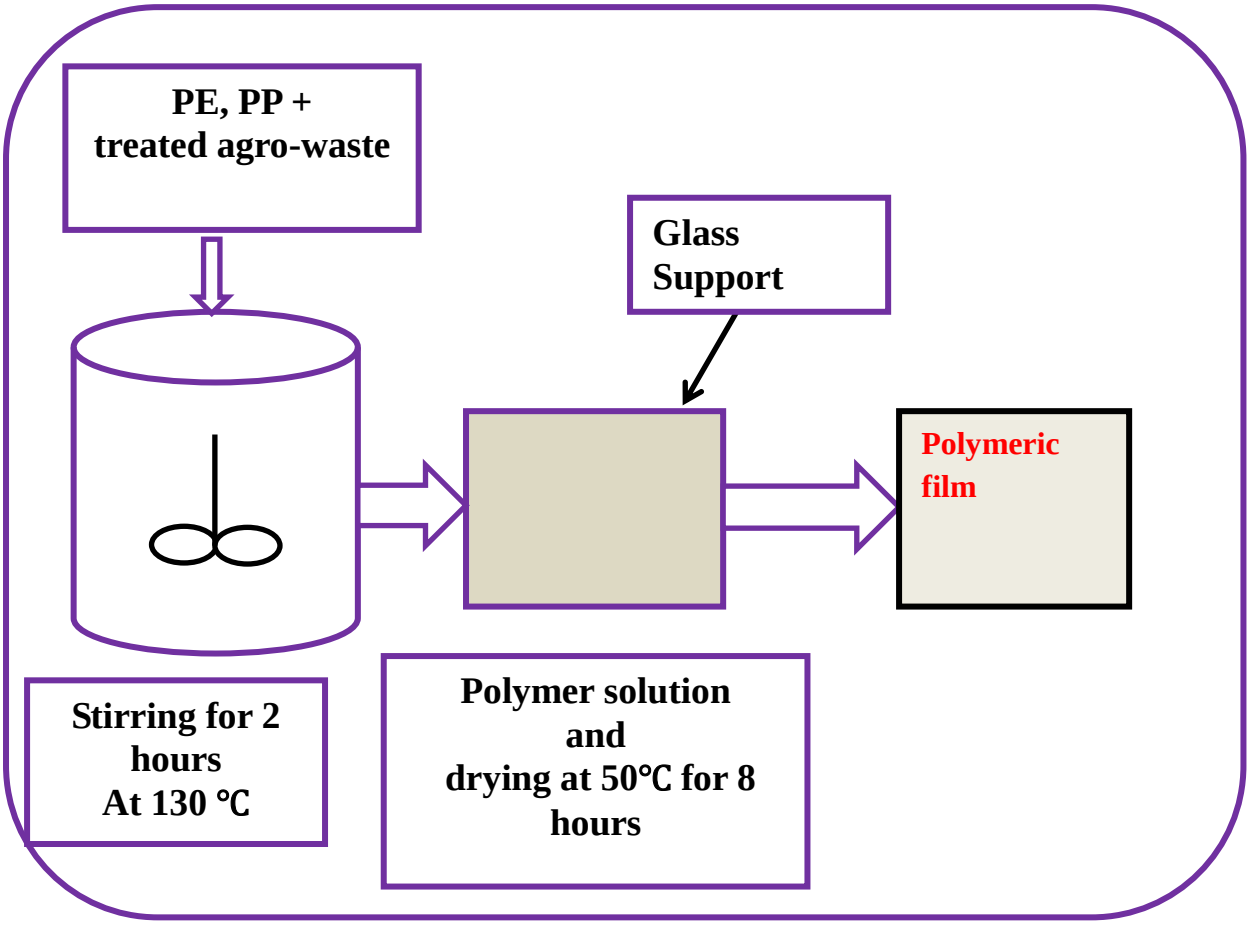

Figure 3.1 Schematic diagram of solvent casting method.

3.2.5 Experimental design and optimization for polyethylene/polypropylene/alkali treated- wheat straw based biocomposite film

In this study, RSM was chosen to determine the favourable condition for the synthesis of PE/PP/alkali treated-wheat straw. RSM has many advantages over conventional methods such as it requires less number of experiments and experimental data, provides optimized parameters, less time consuming and it also holds in cost minimization. All experiments are lined-up on the basis of CCD. CCD provided the two sets of factors such as center points and axial points. In the set of experiments, center points of experiments are generally repeated for maintaining the accuracy of the experiments. Moreover, axial point values are fitting above and below the center points of the two factorial levels (Razali et al., 2013).

A film having high mechanical strength, elongation at break (%) in range and low WVTR was optimized using CCD model. In this experiment, three independent variables existed viz; polyethylene (1.8-1.08 g), polypropylene (1.2-0.72 g) and alkali treated- wheat straw (0-1.2 g). The number of experiments was 20 derived from the following equation 2(Tan et al., 2008).

$$N = 2^n + 2n + n_c \quad (2)$$

where number of independent variables (n) was 3, number of replicates at central points (n_c) was 6 and thus total number of experiments was 20.

Table 3.1 and Table 3.2 depict a CCD for PE/PP/Alkali treated-WS biocomposite film prepared by using Stat-Ease Design-Expert design expert software (version-11). The experimentally calculated actual value was closer to the predicted value given by design software proving the reliability of RSM. Tensile strength represents the mechanical stability of a biocomposite film, elongation at break (%) exhibits the flexibility of a

biocomposite film and WVTR signifies the water vapor migration rate through the film for packaging application. Responses obtained from experiments were used for the optimization of the independent variables. In order to optimize the parameters, the second order polynomial equation was applied from CCD model. The general mathematical form of the second order equation is shown in the following equation 3.

$$Y = b_0 + \sum_{i=1}^{k} b_i X_i + \sum_{i=1}^{k} b_{ij} X_i^2 + \sum_{i_{i>j}}^{k} \sum_{j}^{k} b_{ij} X_i X_j + \varepsilon \quad (3)$$

Where b_0 represents the regression coefficient, k represents the number of parameters used in CCD model, i represent the linear coefficient, j represents the quadratic coefficients and ε represents the random error.

In order to check the reliability of the mathematical equation provided by RSM, analysis of variance (ANOVA) was used. This ANOVA analysis inspected the suitability of the polynomial second order equation using several factors like determination coefficient (R^2), adjusted determination of coefficient (R^2_{adj}), F value, p-value, degree of freedom (DF) to examine the statistical fitness of the CCD model. The value of p less than 0.05 is indicating a well-suited model for the experiments. The 3-D graphical plots also illustrate the individual and mutual effects of the independent variables on tensile strength, elongation at break (%) and WVTR of PE/PP/Alkali treated-WS biocomposite film.

Table 3.1 Variables used in the experimental design represented with actual and coded values.

Variables	Symbol	Coded level		
		-1	**0**	**+1**
Polyethylene	PE	1.08 g (25.71%)	1.44 g (34.28%)	1.8g (42.85%)
Polypropylene	PP	0.72 g (17.14%)	0.96 g (22.85%)	1.2 g (28.51%)
Alkali-treated-wheat straw	Alkali-treated-WS	0	0.6 g (14.28%)	1.2 g (28.51%)

Table 3.2 Experimental design matrix for PE/PP/alkali treated-WS composite film with responses.

Run	A:Polyethylene	B:Polypropylene	C:Alkali treated-WS	Tensile strength (MPa)		Elongation at break (%)		WVTR ($g.m^{-2}.day^{-1}$)	
				Actual Value	**Predicted Value**	**Actual Value**	**Predicted Value**	**Actual Value**	**Predicted Value**
1	-1	-1	+1	41.00	41.04	123.00	123.03	70.00	69.40
2	-1	-1	0	39.00	38.43	125.00	124.65	63.00	62.71
3	0	-1	0	39.50	39.35	124.00	124.37	57.50	58.42
4	-1	+1	+1	39.50	39.99	123.50	123.68	63.00	63.27
5	-1	-1	+1	43.00	43.09	120.00	120.03	59.00	58.84
6	0	-1	-1	36.00	36.33	126.00	125.95	56.25	55.11
7	0	-1	0	39.12	39.35	124.30	124.37	59.00	58.42
8	-1	+1	+1	45.00	45.04	120.00	119.93	52.00	51.73
9	0	-1	0	39.10	39.35	125.00	124.37	58.50	58.42
10	-1	-1	0	42.00	42.23	125.00	125.15	55.00	54.92
11	-1	+1	-1	41.00	41.04	128.00	128.03	51.25	51.94
12	0	-1	+1	43.00	42.33	121.00	120.85	60.00	60.77
13	-1	-1	0	36.00	35.59	130.00	129.88	54.00	53.83
14	0	+1	0	40.00	39.43	124.50	124.35	57.00	56.06
15	0	-1	0	38.50	39.35	124.20	124.37	59.00	58.42
16	-1	-1	-1	33.00	33.04	125.00	125.13	57.50	57.87
17	-1	+1	-1	35.50	35.49	124.00	124.03	56.70	56.96
18	0	-1	0	39.40	39.35	123.70	124.37	57.25	58.42
19	0	-1	0	37.00	37.23	125.00	124.95	59.50	60.07
20	0	-1	0	39.80	39.35	124.60	124.37	58.50	58.42

3.2.6 Characterization of native and pre-treated-wheat straw

3.2.6.1 XRD analysis

The crystalline changes in native-WS and alkali treated-WS were studied using X-ray diffractometer (XRD, model mini flux II, Rigaku, Japan) with a scanning rate of 5^o per minute in the range of 0^o to 70^o (2θ) along with wavelength 1.54060 A^o.

3.2.6.2 FTIR analysis

To study the functional groups, present in biomass, FTIR analysis of native-WS and alkali treated-WS was recorded using Thermo-Nicolet 5700 (Waltham, United States) technique in transmittance mode. FTIR spectra were obtained in a range of 4000-400 cm^{-1} wavenumber in this analysis with a resolution of 4 cm^{-1}.

3.2.6.3 Compositional analysis

To study the percentage removal of hemicellulose and lignin from agro-waste, the compositional analysis of agro-waste was performed. Holocellulose, hemicellulose, cellulose and lignin contents of agro-waste and alkali treated-agro-waste were calculated (Bledzki et al., 2010).

3.2.6.4 SEM analysis

The surface morphology analysis of native-WS and alkali treated-WS was studied using scanning electron microscopy (SEM, model JEOL JSM5410, Japan). A gold coating was done on the polymeric composite sample to make our sample conductive for further analysis with an accelerating voltage of 20KV.

3.2.7 Characterization of polyethylene/polypropylene/alkali treated-wheat straw bio-composite film

3.2.7.1 SEM analysis

The surface morphology of PE/PP, PE/PP/Native-wheat straw and PE/PP/Alkali treated- WS composite films was analysed using SEM analysis (EVO - Scanning Electron Microscope MA15 / 18, CARL ZEISS MICROSCOPY LTD., USA) at a 20kV voltage with 500 X magnification. In the sample preparation process, initially, the gold coating was done on the film to make it conductive for SEM analysis.

3.2.7.2 FTIR analysis

FTIR spectra of all prepared composite films were obtained using Thermo Scientific iD7 ATR technique. Samples were analysed using transmittance mode from 400 to 4000 cm^{-1} wavelength with a 45^{O} ZeSe crystal.

3.2.7.3 XRD analysis

The XRD analysis of PE/PP, PE/PP/Native-wheat straw and PE/PP/Alkali treated- WS composite films was performed using an X-ray diffractometer (XRD, model mini flux II, Rigaku, Japan) with a Cu K_{α} radiation (λ = 0.154 nm). The XRD was conducted at 2 theta values of 5^{o}- 70 ^{o} with a scanning rate of 5^{o}/min at 40 kV operating voltage (Perumal et al., 2018).

3.2.7.4 TGA analysis

TGA analysis provides information about the thermal stability of a film over time as temperature changes. The thermal stability of polymeric composite film was observed using a PerkinElmer instrument, USA. In this analysis, the composite film was heated from room temperature to 600 ^{o}C at a heating rate of 10 ^{o}C/min under a nitrogen atmosphere.

3.2.7. 5 Mechanical tests

The mechanical strength such as tensile strength, elongation at break (%) and tensile modulus of PE/PP, real polyethylene packaging, real polyester packaging, PE/PP/Native-wheat straw and PE/PP/Alkali treated-WS composite films were determined using the universal testing machine (INSTRON 5982 Floor Model System, US). The mechanical testing was performed using ASTM D0882 having gauge length 5mm with testing speed 30mm/min (Haddar et al., 2018). The thickness of the films was 0.25±0.2 mm.

3.2.7.6 Contact angle measurement

In order to signify the water-resistant property of the film, the water contact angles of PE/PP, real polyethylene packaging, real polyester packaging, PE/PP/Native-wheat straw and PE/PP/Alkali treated- WS composite films were examined by using the sessile drop method (KRUSS DSA25 Series, Germany) at room temperature. In this measurement, the droplet of water was placed on the film surface and the droplet was allowed to expand on the film surface for 1 s. Subsequently, water contact angle of the film was recorded. This procedure was repeated 5 times and the average value of the contact angle was calculated (Simmons et al., 2016; Tsuchiya et al., 2019).

3.2.7. 7 WVP test

In this test, WVTR of PE/PP, real polyethylene packaging, real polyester packaging, PE/PP/Native-wheat straw and PE/PP/Alkali treated- WS composite films were determined. Initially, a wet chamber was prepared by a glass beaker tightly covered with bio-composite film. Subsequently, the weight of the wet chamber was measured and it was placed in an incubator at 23 ^{o}C. The relative humidity of the incubator was maintained at 53-55%. Moreover, the change in weight of bio-composite film was observed regularly at an interval of 24 hrs. Based on the weight loss through the film,

WVTR was calculated using the following equation 4 (Râpă et al., 2016; Sirviö et al., 2014).

$$WVTR = \frac{WC1-WC2}{WC1*A*day} \quad (4)$$

Where WC1 and WC2 represent the initial and final weight of the wet chamber and A represents the exposed area of the wet chamber.

Water vapor permeation rate is also calculated using following equation.

$$WVPR = \frac{WVTR*T}{S(R1-R2)} \quad (5)$$

Where S is a saturation vapor pressure at 23 ^{o}C (2800 Pa), R1 is the relative humidity of the inside wet cup chamber, R2 is the relative humidity of incubation chamber and T is the thickness of a film (m).

3.2.7. 8 Dart Impact test

Dart impact tester is generally used to calculate the impact strength of the polymeric film and evaluating films suitability for packaging applications. Impact strength is an essential characteristic for visualizing the stiffness of the film which provides detailed information about impact energy and impact force using a free-falling dart impact method. Moreover, this property plays a crucial part as the material will be exposed to impact during transportation. ASTM D1709 is suitable for measuring the dart impact strength of the film. Impact test for all prepared composite films was performed using Dart Impact tester (Asian Test Equipments, Hapur, India) with 2.93 m/s striking velocity before impact. The films were cut in the size of 220mm X 220mmX 0.25mm and the dart of different weights (10 g to 100 g) were dropped from a height (43 cm) for calculating the impact strength.

$$\text{Impact energy } (KE) = \frac{1}{2}\, m\, v^2 \quad (6)$$

$$\text{Impact Force} = \frac{KE}{d} \quad (7)$$

Where m is mass of dart (kg) dropped from certain h (m), and d (m) represents distance travelled after the impact i.e. the thickness of the film.

3.2.7. 9 Optical characteristics test

Transparency test for PE/PP, real polyethylene packaging, real polyester packaging, PE/PP/Native-wheat straw and PE/PP/Alkali treated- WS composite films were analysed using Elico SL 210 UV VIS spectrophotometer. In this test, the film was directly exposed in the spectrophotometer at a visible wavelength of 400-800 nm. Moreover, a blank compartment was also used as a reference in the study (Saha et al., 2018).

3.3 Results and discussion

3.3.1 Characterization of native-WS and alkali treated-WS

In this section, XRD analysis, FT-IR analysis, compositional analysis and SEM analysis for native-WS and alkali treated-WS were studied.

3.3.1.1 XRD analysis

The crystalline changes in the lignocellulosic fiber after pre-treatment are analysed using XRD analytical technique and XRD graph is shown in Figure 3.2. The existence of hydrogen bonds between cellulose which are arranged in an ordered system causes crystalline structure of agro-waste. The major peak for alkali treated and untreated agro-waste exhibited the crystalline areas, which is exploring the presence of cellulosic fibers in agro-waste. The two major peaks are found for untreated and alkali treated agro-waste at different concentrations viz., 1%, 2.5%, 5%, 7.5%, 10% which are at 16° and

22° 2θ. The peak at 16° and 22° 2θ represents (101), (202) planes, respectively which are exhibit cellulose I structure according to JCPDS. No. 03-0226.

The principal broader peak for wheat straw is found at 21.92° for native-WS, 21.77° for 1% NaOH treated-WS, 21.92° for 3% NaOH treated-WS, 22.07° for 5% NaOH treated-WS, 22.08° for 7% NaOH treated-WS, and 22.23° for 10% NaOH treated-WS, respectively. The % crystallinity for native-WS, 1% NaOH treated-WS, 3% NaOH treated-WS, 5% NaOH treated-WS, 7% NaOH treated-WS, and 10% NaOH treated-WS is found to be 40.15, 43.18, 46.14, 49.29, 48.71, 48.14, respectively. An enhanced peak height at 22° represents a higher crystallinity of cellulose present in agro-waste due to a reduction in amorphous region of agro-waste.

An increase in peak height at 22° 2θ reveals successful removal of lignin and hemicellulose from agro-waste. This equivalent result was reported by Pickering et al., 2011 in their published article. Hence, alkali treatment affects amorphous region of lignocellulosic fibers and improves the hydrophobicity of treated-agro-waste for enhancing its suitability for polymer adhesion. Kalia and Vashistha, 2012 explained similar results in their published literature. The higher peak height at 22° 2θ is correlated with higher mechanical strength of treated-agro-waste (Alemdar and Sain, 2008).

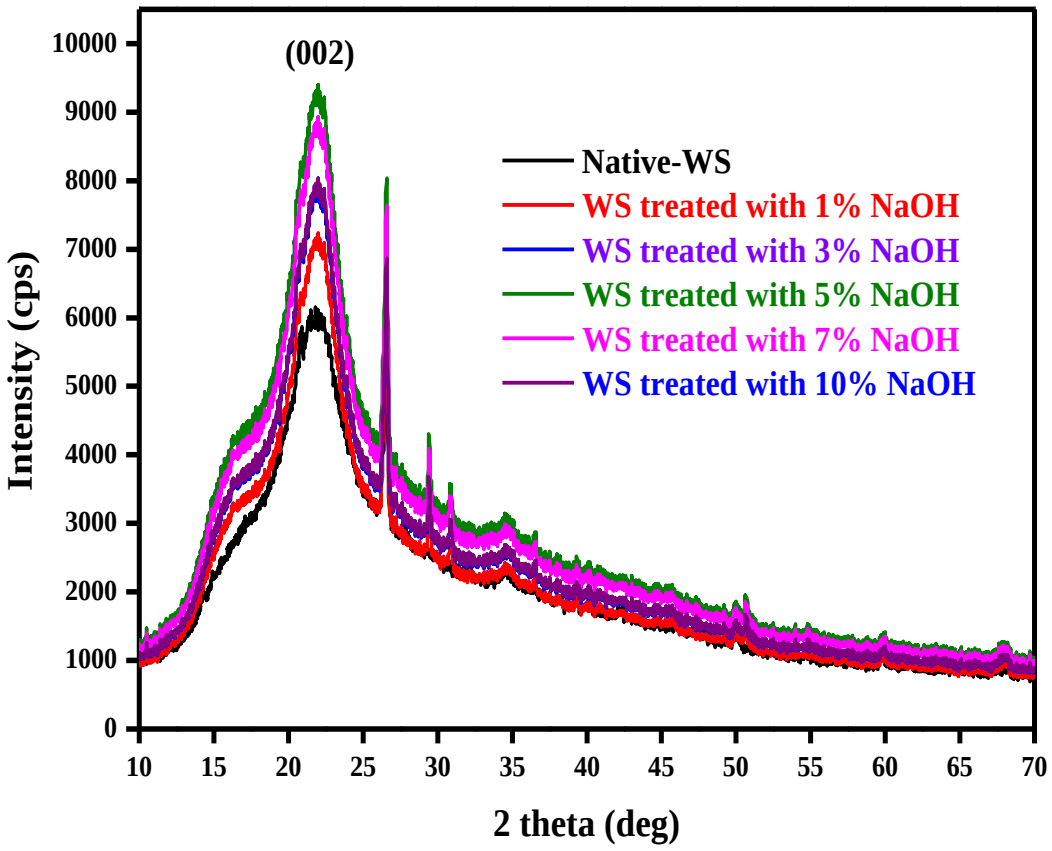

Figure 3.2 XRD analyses for native- wheat straw and alkali treated- wheat straw.

3.3.1.2 FTIR analysis

FTIR is an imperative method that provides information about various functional groups present in a material. The structural changes in the wheat straw after alkali treatment were analysed using FTIR technique in the wavelength range of 3500-600 cm^{-1} for visualizing the structural information of the wheat straw and alkali treated-wheat straw. The impact of various concentrations of NaOH viz., 1%, 2.5%, 5%, 7.5%, 10% on agro-waste depicted in the Figure 3.3.

Peak at 1550-1610 cm^{-1} represents a carboxylic functional group or hemicellulose present in the biomass (Tang et al., 2015). Therefore, that peak decreases after pre-treatment with a higher concentration of NaOH showing degradation of hemicellulose in the treated-biomass. Peak at 1220-1260 cm^{-1} signifies the acetyl functional group present in the agro-waste. Peak at 1400-1500 cm-1 shows aromatics (lignin) existing in the biomass that is also decreasing in FTIR spectra of treated-WS (Laadila et al., 2017). C-H stretching assigned to peak at 2850-3000 confirms cellulose present in the agro-waste. This peak appears more effective after pre-treatment and reveals the significant decrement in the percentage of hemicellulose and lignin in the treated-WS. This result shows compatibility with the published article (Cao and Tan, 2004). Peak at 2900-3400 cm^{-1} assigned to hydroxyl groups in biomass is continuously decreasing at higher concentrations of NaOH treatment revealing reduction of hydroxyl groups. This depicts the effectiveness of alkali treatment on agro-waste and also indicates enhanced moisture resistance characteristics of biomass.

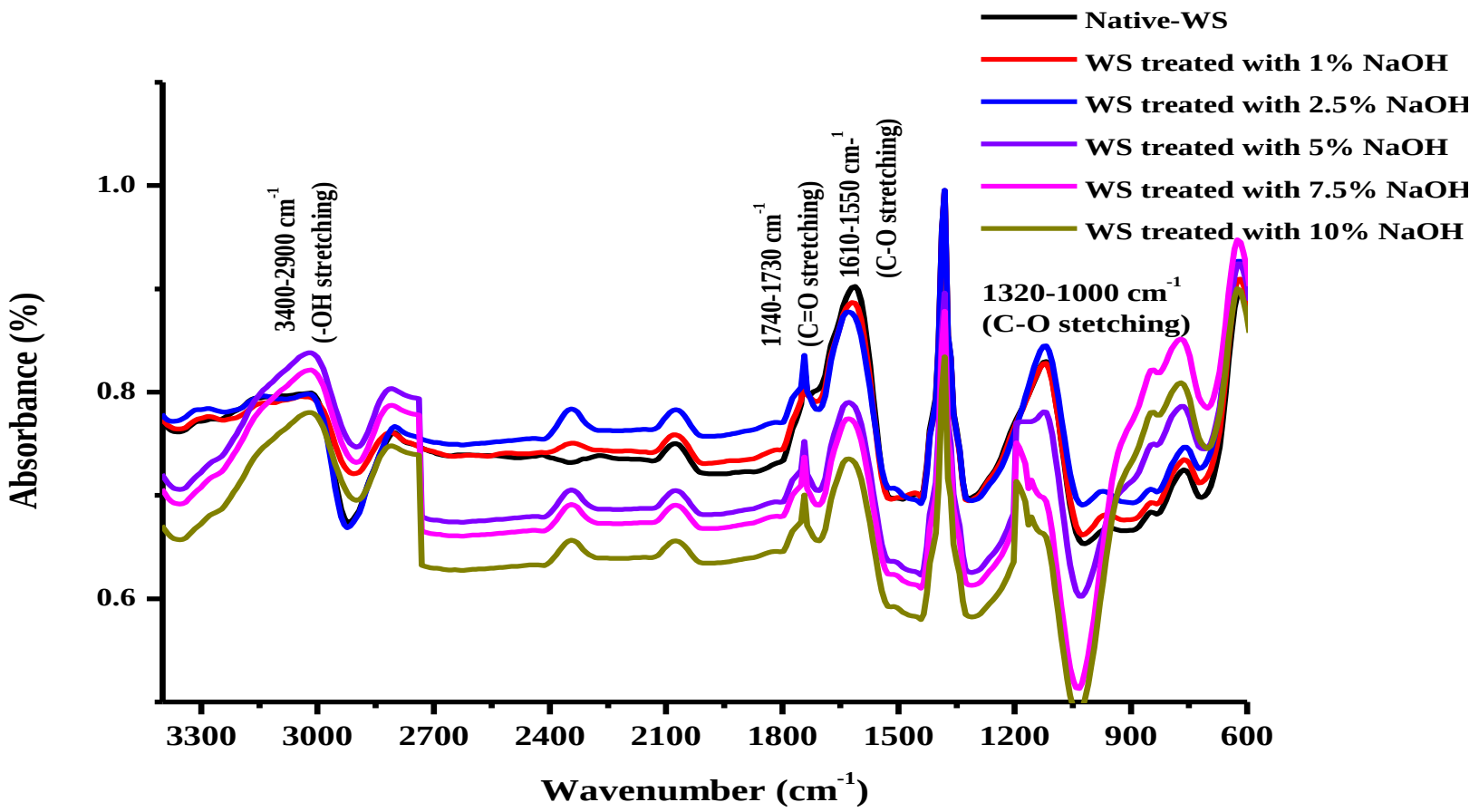

Figure 3.3 FTIR analyses for native-wheat straw and alkali treated- wheat straw.

3.3.1.3 Compositional analysis

Compositional analysis of native-agro-waste and NaOH treated- agro-waste is depicted in Table 3.3. Generally, hemicellulose exhibits xylose, mannose and arabinose contents present in the biomass. Lignin is an insoluble resin material of phenolic characteristics. Holocellulose content is a summation of hemicellulose and cellulose present in the biomass (Bledzki et al., 2010).

In alkali treatment of wheat straw, hemicellulose and lignin contents are reduced from 29% to 17% and 16% to 2.72 % which is surging the cellulose percentage in the biomass. But at higher concentration of NaOH (greater than 5%), cellulose started to degrade in agro-waste. So Holocellulose content is decreased at higher concentration of alkali. Similar results surveyed by authors in their article (Agbor et al., 2011).

Table 3.3 Compositional analyses for native-WS and alkali treated-WS**.**

Agro-waste	**Lignin (%)**	**Holocellulose (%)**	**Hemicellulose (%)**	**Cellulose (%)**
Native-WS	16	63	29	34
WS treated with 1% NaOH	8	71	22.91	48.09
WS treated with 3% NaOH	4.96	74.04	19.41	54.63
WS treated with 5% NaOH	2.72	76.28	17	59.28
WS treated with 7% NaOH	4.81	74.19	17.40	56.79
WS treated with 10% NaOH	6.09	72.91	17.16	55.75

3.3.1.4 SEM analysis

In order to elucidate the surface topography of untreated and treated agro-waste, SEM analysis is performed. The roughness changes in the surface of treated-agro-waste at optimized NaOH concentration are depicted in Figure 3.4. After pre-treatment with optimized alkali concentration, the change in surface morphology of agro-waste was analysed by SEM to obtain the structural modification of the surface.

The surface images of Native-WS and alkali treated-WS are shown in Figure 3.4 with a magnification of 2.00 kx with 20.0 kV voltage. In the native-WS, the surface is containing impurities and some components are expected to be residual lignin. This shows hindrance to obtain better interfacial interactions for polymer adhesion. Figure reveals the destruction of plant cells, which results in irregular shape having many filaments, cells and pores. Voids were present at the surface of biomass confirm that the sample morphology was very suitable for adhesion between wheat straw and polymer matrix. It also indicates that for pre-treated wheat straw with optimized alkali concentration, there is a decrease in resistant nature of wheat straw by increasing the cellulose digestibility.

Rough surface with many impurities have also been reported in previous studies (Asumani et al., 2012; Lee et al., 2013). The surface appears rough with some void openings exhibiting an elimination of lignin and hemicellulose from agro-waste. The formation of some voids at the surface representes the destruction of the external wall of agro-waste. This destruction of the outer wall is correlated with the suitability of fiber for polymer adhesion. Luo et al., 2014 prepared treated-corn fiber/polylactic composites and stated equivalent outcomes in their published article.

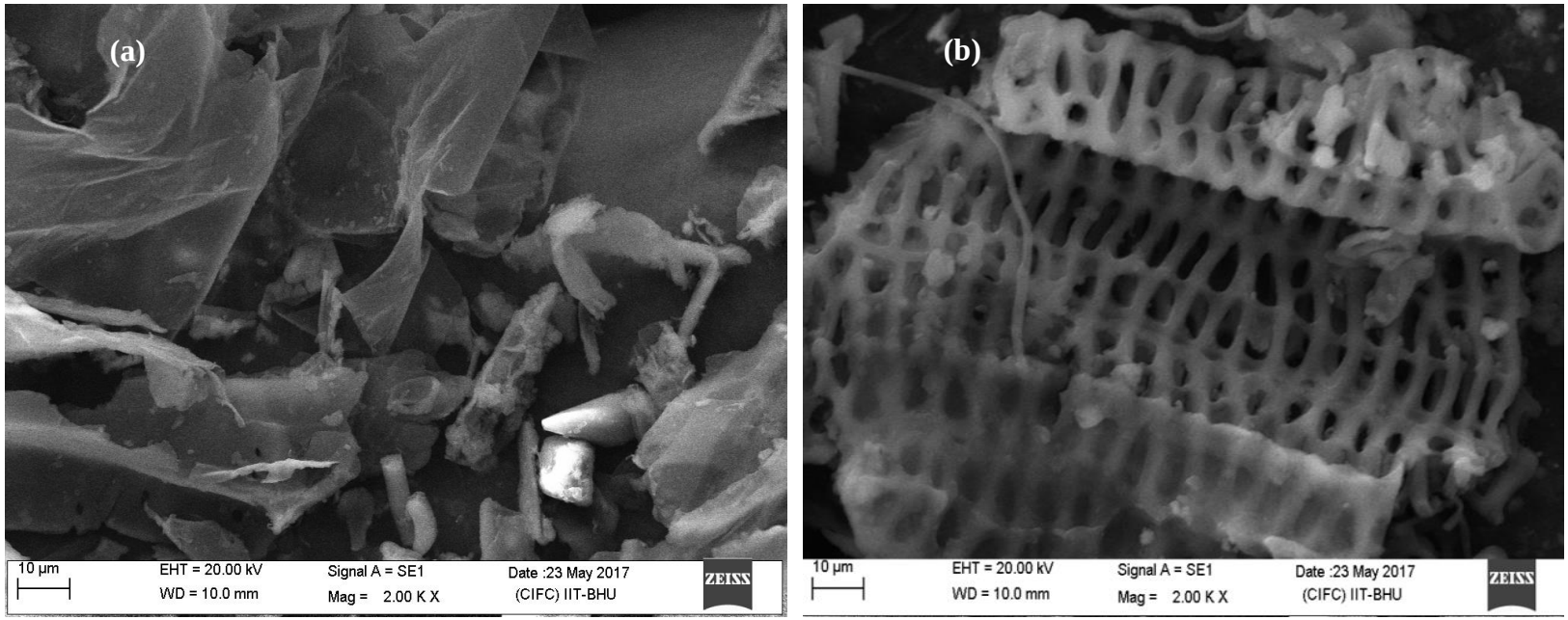

Figure 3.4 SEM analyses for native and alkali treated- wheat straws (a) Native-WS (b) Alkali treated-WS.

3.3.2 RSM and ANOVA analysis

3.3.2.1 ANOVA and RSM analysis for tensile strength, Elongation at break and WVTR of PE/PP/Alkali treated-WS biocomposite film

3.3.2.1.1 Data adequacy check of the Model

After conducting the set of experiments provided by RSM, the resultant data were analysed using ANOVA analysis. Figure 3.5 exhibits the actual and predicted responses such as tensile strength, elongation at break (%) and WVTR in which actual values are dependent variable data of specific experiment and the predicted values were provided by the RSM model. Figure reveals that all points lie around the diagonal line in the graph of predicted value vs. actual value. According to Lu et al., 2009, variable data points lying on the straight line suggest the adequacy of the model. This behaviour of the graph represents that the results fit well with the predicted value. The higher R^2 value 0.9820 for tensile strength, 0.9870 for elongation at break (%) and 0.9768 for WVTR assure the reliability of the model. These outcomes are similar to the results reported by Satapathy and Das, 2014.

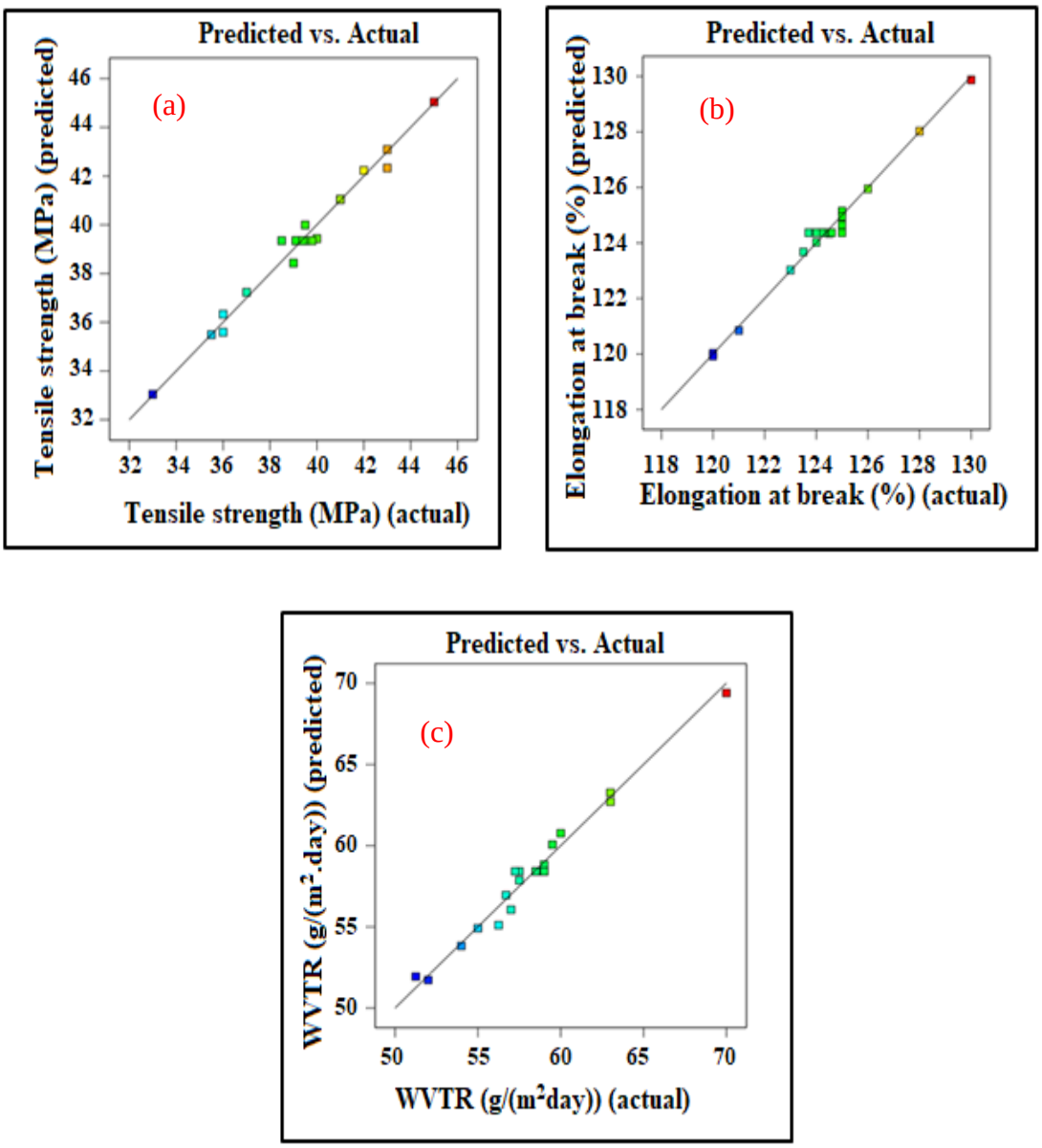

Figure 3.5 Relationship between actual and predicted values of model (a) Tensile strength and (b) Elongation at break (%) (c) Water vapor transmission rate.

3.3.2.1.2 Effect of process variables on Tensile strength

The RSM model for the tensile strength of the biocomposite film is shown in following equation.

$$Y_{TS} = + 31.71964 - 24.50631\ A + 29.69886\ B + 11.73030C + 8.68056AB - 0.578704\ AC - 6.07639\ BC + 7.56874\ A^2 - 17.69255\ B^2 - 0.053030C^2 \quad (8)$$

Where linear terms (A, B, C), interaction terms (AB, BC, AC) and quadratic terms (A^2, B^2, C^2), are there in the mathematical equation. According to ANOVA analysis, all the factors followed the second-order quadratic model for tensile strength. The p value<0.05 and higher F value signify the suitability of the model. Value of $p < 0.0001$and the F-value of 60.67 indicate that the model is well suited to the experiments (Table 3.4). A p-value is generally expressing the probability of error that is correlated with the validation of the observed result (Xiangli et al., 2008). The p-value for linear terms, interaction term, and quadratic terms are less than 0.05 showing the benchmark impact of process parameters on tensile strength. The standard deviation of the model is found to be 0.5293. Hence it can be concluded that the results show the reliability of the RSM model.

3-D graphical response plots illustrate the interactions between the independent variables and dependent variables for tensile strength (Figure 3.6). Figure 3.6(a) reveals that at low and high concentration of polypropylene, tensile strength continuously increases with the polyethylene concentration (1.08 g to 1.8g). This signifies the remarkable effect of polyethylene on tensile strength. Similar behaviour is illustrated from the interaction pattern of polyethylene and alkali treated-WS (Figure 3.6(c)), and polypropylene and alkali treated-WS (Figure 3.6(e)) for tensile strength of

biocomposite film. These results assure the considerable interaction of independent parameters for optimization of the tensile strength of biocomposite film and also encourage the use of alkali treated-WS in the synthesis of composite film for packaging applications.

Table 3.4 ANOVA analysis for the tensile strength of PE/PP/alkali treated-WS from CCD model.

Source	**Sum of Squares**	**df**	**Mean Square**	**F-value**	**p-value**	
Model	152.96	9	17.00	60.67	< 0.0001	significant
A-Polyethylene	36.10	1	36.10	128.86	< 0.0001	
B-Polypropylene	12.10	1	12.10	43.19	< 0.0001	
C-Alkali treated-WS	90.00	1	90.00	321.25	< 0.0001	
AB	4.50	1	4.50	16.06	0.0025	
AC	0.1250	1	0.1250	0.4462	0.5193	
BC	6.13	1	6.13	21.86	0.0009	
A^2	2.65	1	2.65	9.44	0.0118	
B^2	2.86	1	2.86	10.19	0.0096	
C^2	0.0010	1	0.0010	0.0036	0.9535	
Residual	2.80	10	0.2802			
Lack of Fit	1.81	5	0.3626	1.83	0.2608	not significant
Pure Error	0.9883	5	0.1977			
Cor Total	155.76	19				
Std. Dev.	0.5293		**R^2**	0.9820		
Mean	39.32		**Adjusted R^2**	0.9658		
C.V. %	1.35		**Predicted R^2**	0.8950		
			Adeq Precision	32.0625		

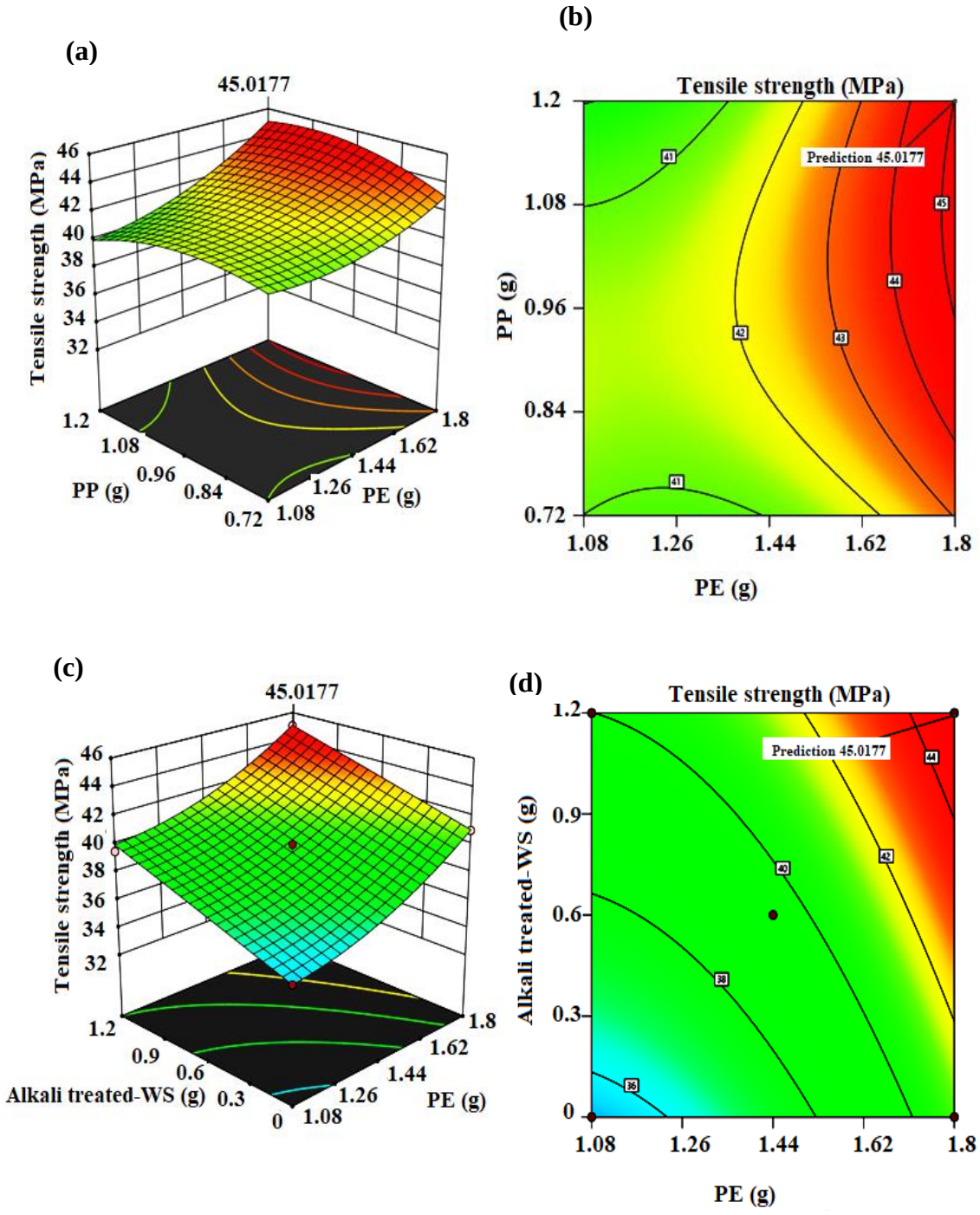
(a)
45.0177
Tensile strength (MPa)
46
44
42
40
38
36
34
32
1.2
1.08
0.96
0.84
0.72
PP (g)
1.08
1.26
1.44
1.62
1.8
PE (g)
(b)
Tensile strength (MPa)
Prediction 45.0177
41
42
43
44
45
PP (g)
1.2
1.08
0.96
0.84
0.72
1.08
1.26
1.44
1.62
1.8
PE (g)
(c)
45.0177
Tensile strength (MPa)
46
44
42
40
38
36
34
32
1.2
0.9
0.6
0.3
0
Alkali treated-WS (g)
1.08
1.26
1.44
1.62
1.8
PE (g)
(d)
Tensile strength (MPa)
Prediction 45.0177
36
38
40
42
44
Alkali treated-WS (g)
1.2
0.9
0.6
0.3
0
1.08
1.26
1.44
1.62
1.8
PE (g)

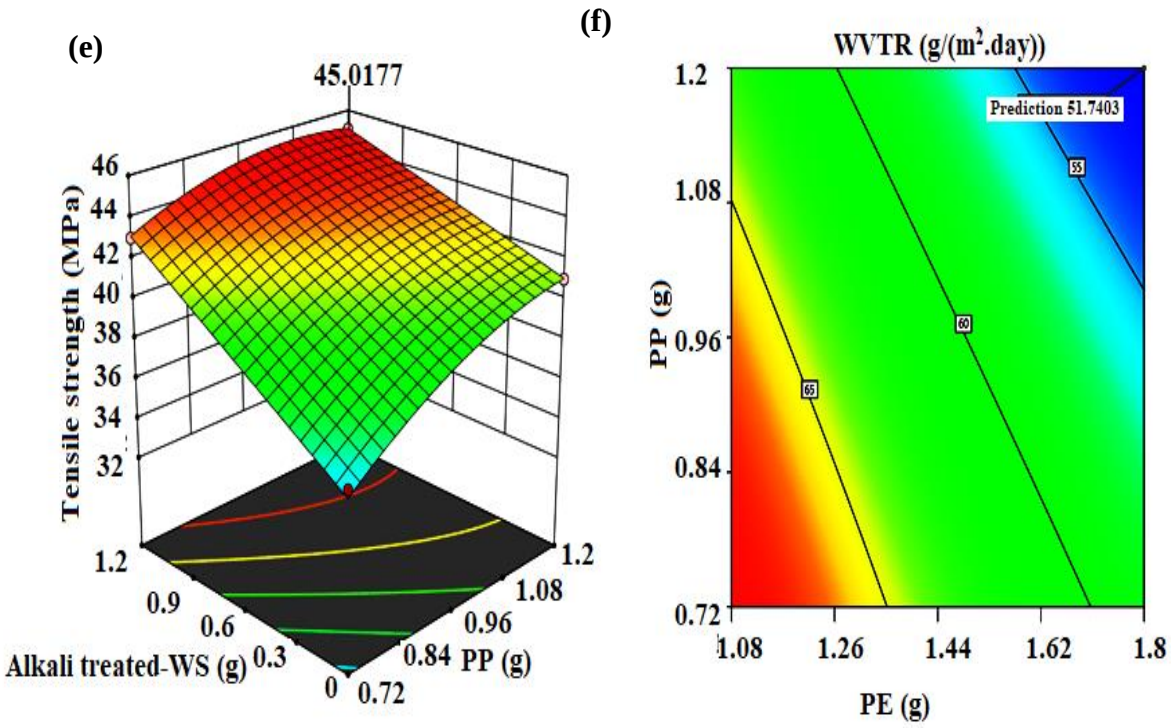

Figure 3.6 Three-dimensional response surface and contour plots of tensile strength showing the effect of (a) and (b) polypropylene and polyethylene; (c) and (d) alkali treated-WS and polyethylene; (e) and (f) alkali treated-WS and polypropylene.

3.3.2.1.3 Effect of process variables on Elongation at break (%)

The statistical equation for elongation at break (%) of bio-composite film is shown in the following equation.

$$Y_{EA}= +130.16727-3.65846A -9.34186B +8.97727C -2.17014AB -8.96991AC+3.03819 BC+4.10354A^2+4.89268B^2-2.68939C^2 \quad (9)$$

ANOVA analysis provides a significant model of p-value < 0.0001 and F value 84.22 for elongation at break (%) of the bio-composite film. In this analysis, p-value≤0.05 for linear term (A, B, C), interaction term (AC, BC) and quadratic term (A^2, C^2) assures the remarkable impact of these independent variables on elongation at break (%) of PE/PP/Alkali treated-WS biocomposite film and thus proving the suitability of CCD model (Table 3.5).

Figure 3.7 represents the 3-D plots of the independent and dependent variables for elongation at break (%) of biocomposite. At low and high concentration of polypropylene, there is a decrease in elongation at break (%) with increasing the concentration of polyethylene from 1.08 g to 1.8 g (Figure 3.7(a)). The same pattern was found in the case of polyethylene and alkali treated-WS in RSM plot for elongation at break (%) of biocomposite film (Figure 3.7(c)). But on the other hand, the interaction pattern of polypropylene and alkali treated-WS exhibits that at high and low concentrations of alkali treated-WS, there is no significant influence on elongation at break (%) at certain concentration of polypropylene (Figure 3.7(e)). Thus, it can be concluded that the value of elongation at break (%) is found to be in a range (120-125%) with the addition of alkali treated-WS in the composite film for packaging applications.

Table 3.5 ANOVA analysis for elongation at break (%) of PE/PP/alkali treated-WS from CCD model.

Source	**Sum of Squares**	**df**	**Mean Square**	**F-value**	**p-value**	
Model	101.06	9	11.23	84.22	< 0.0001	significant
A-Polyethylene	0.6250	1	0.6250	4.69	0.0556	
B-Polypropylene	0.9000	1	0.9000	6.75	0.0266	
C-Alkali Treated biomass	65.02	1	65.02	487.68	< 0.0001	
AB	0.2812	1	0.2812	2.11	0.1770	
AC	30.03	1	30.03	225.23	< 0.0001	
BC	1.53	1	1.53	11.48	0.0069	
A^2	0.7778	1	0.7778	5.83	0.0364	
B^2	0.2184	1	0.2184	1.64	0.2295	
C^2	2.58	1	2.58	19.33	0.0013	
Residual	1.33	10	0.1333			
Lack of Fit	0.2933	5	0.0587	0.2821	0.9045	not significant
Pure Error	1.04	5	0.2080			
Cor Total	102.40	19				
Std. Dev.	0.3651		**R^2**	0.9870		
Mean	124.29		**Adjusted R^2**	0.9753		
C.V. %	0.2938		**Predicted R^2**	0.9632		
			Adeq Precision	38.5361		

(a)

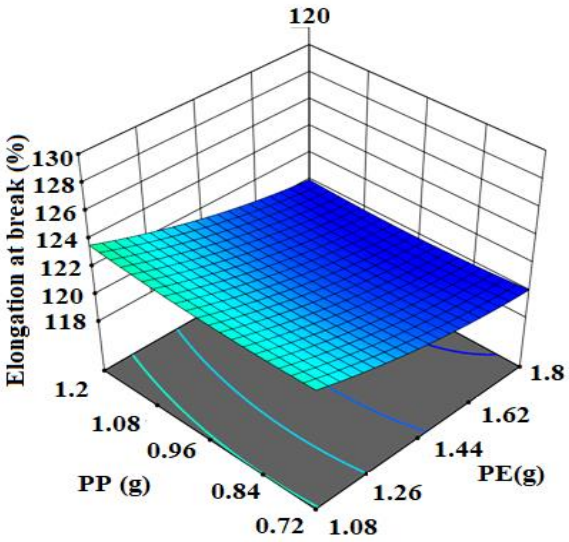
120
Elongation at break (%)
130
128
126
124
122
120
118
1.2
1.08
0.96
0.84
0.72
PP (g)
1.08
1.26
1.44
1.62
1.8
PE(g)

(b)

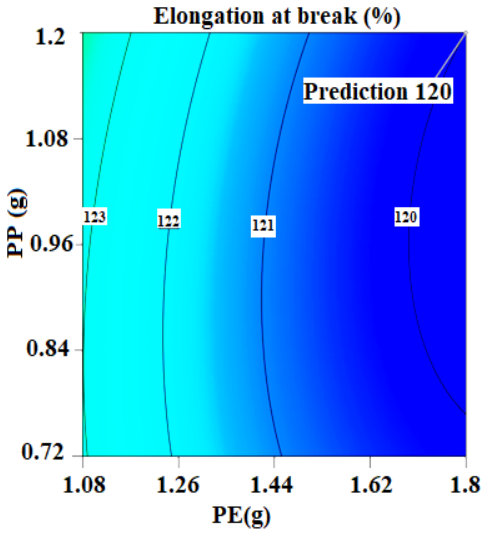
Elongation at break (%)
Prediction 120
1.2
1.08
0.96
0.84
0.72
PP (g)
123
122
121
120
1.08
1.26
1.44
1.62
1.8
PE(g)

(c)

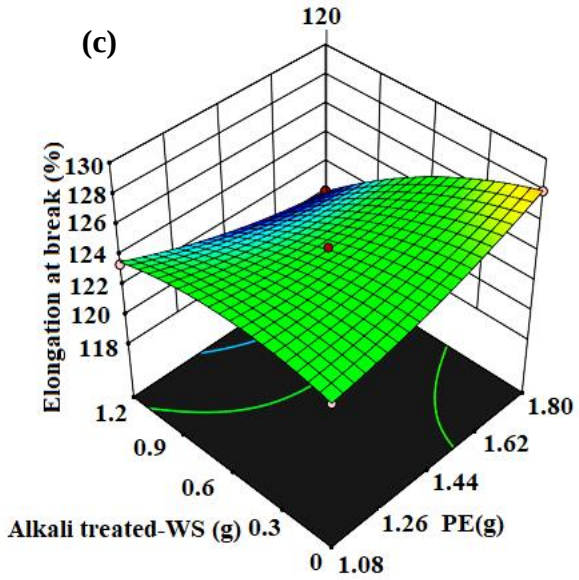
120
Elongation at break (%)
130
128
126
124
122
120
118
1.2
0.9
0.6
0.3
0
Alkali treated-WS (g)
1.08
1.26
1.44
1.62
1.80
PE(g)

(d)

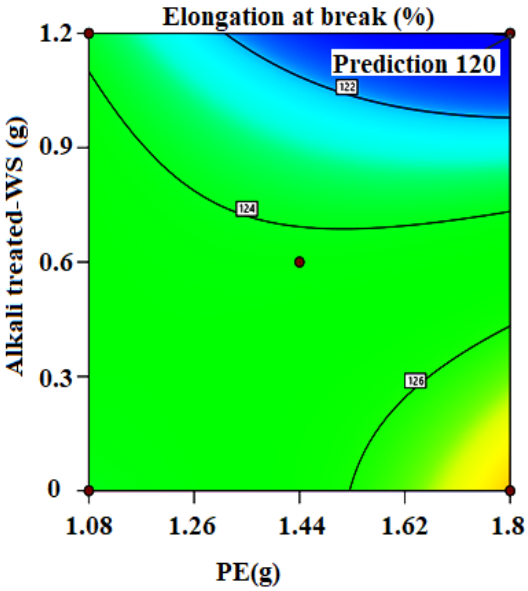
Elongation at break (%)
Prediction 120
122
124
126
1.2
0.9
0.6
0.3
0
Alkali treated-WS (g)
1.08
1.26
1.44
1.62
1.8
PE(g)

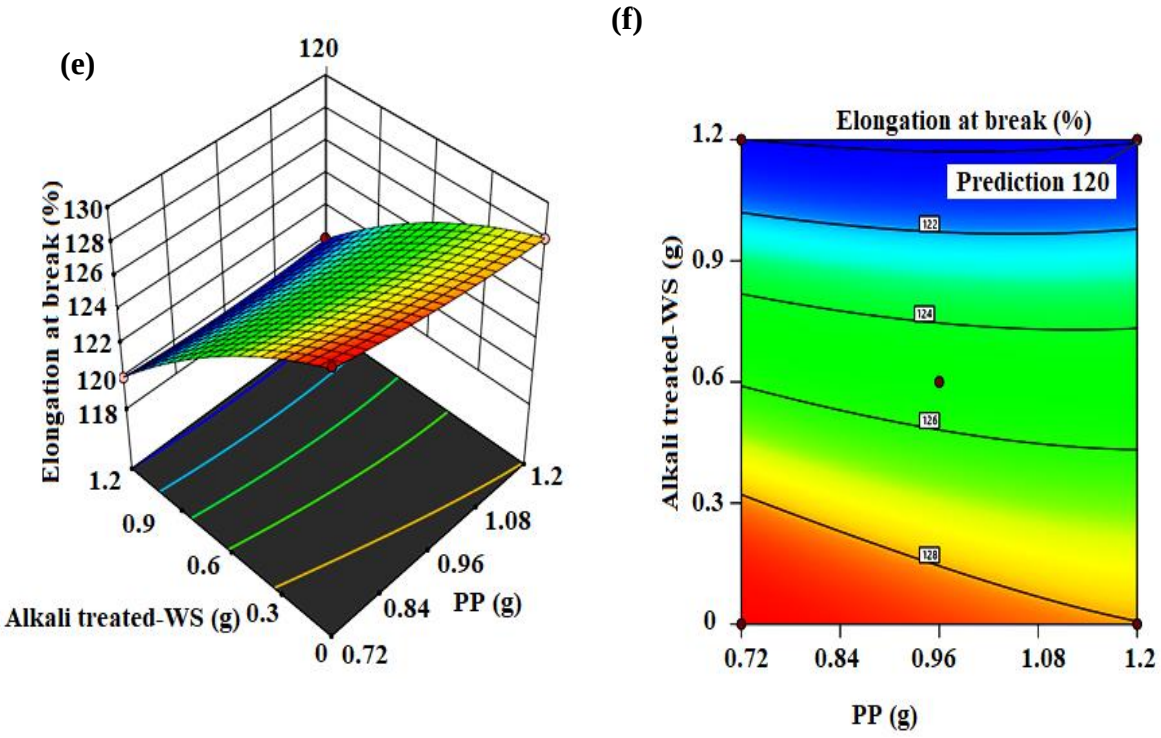

Figure 3.7 Three-dimensional response surface and contour plots of elongation at break showing the effect of (a) and (b) polypropylene and polyethylene; (c) and (d) alkali treated-WS and polyethylene; (e) and (f) alkali treated-WS and polypropylene.

3.3.2.1.4 Effect of process variables on WVTR

RSM model suggests the following equation which optimizes the process parameters for WVTR of PE/PP/Alkali treated-WS biocomposite film.

$$Y_{WVTR} = + 63.71182 - 12.36774\ A + 12.96922\ B + 25.89845C - 2.82118AB - 7.55208AC - 9.07118\ BC + 3.05135\ A^2 - 6.15530\ B^2 - 1.33207C^2 \quad (10)$$

The statistical equation provided by ANOVA analysis shows p value<0.05 and higher F value (46.82) assuring the suitability of the model for WVTR. The p value<0.05 of individual process variables (A, B, C) and interaction process variables (AC, BC) signify the role of independent variables on WVTR of PE/PP/Alkali treated-WS biocomposite film for optimization of the process model (Table 3.6).

Response surface plots for water vapor transmission rate are shown in Figure 3.8. A desirable decrement in WVTR is observed in the interaction pattern of polyethylene and polypropylene as shown in Figure 3.8(a). This result indicates that a higher concentration of polypropylene and polyethylene is correlated with the lower water vapor transmission rate of the composite film. Similar patterns of interaction patterns are observed for polyethylene and alkali treated-WS, and for polypropylene with alkali treated-WS for WVTR (Figure 3.8(c) and Figure 3.8(e)). At lower and higher concentrations of polyethylene and polypropylene, WVTR continuously decreases with surging the contribution of alkali treated-WS in the composite film. So probably, this outcome assures the successful substitution of Polymer with alkali treated-WS for packaging applications.

Table 3.6 ANOVA analysis for water vapor transmission rate of PE/PP/alkali treated-WS from CCD model.

Source	Sum of Squares	df	Mean Square	F-value	p-value	
Model	309.01	9	34.33	46.82	< 0.0001	significant
A-Polyethylene	151.71	1	151.71	206.88	< 0.0001	
B-Polypropylene	40.20	1	40.20	54.82	< 0.0001	
C-Alkali Treated biomass	80.09	1	80.09	109.22	< 0.0001	
AB	0.4753	1	0.4753	0.6482	0.4395	
AC	21.29	1	21.29	29.03	0.0003	
BC	13.65	1	13.65	18.61	0.0015	
A^2	0.4301	1	0.4301	0.5865	0.4615	
B^2	0.3457	1	0.3457	0.4714	0.5080	
C^2	0.6324	1	0.6324	0.8624	0.3749	
Residual	7.33	10	0.7333			
Lack of Fit	4.53	5	0.9062	1.62	0.3054	not significant
Pure Error	2.80	5	0.5604			
Cor Total	316.35	19				
Std. Dev.	0.8563		**R^2**	0.9768		
Mean	58.20		**Adjusted R^2**	0.9560		
C.V. %	1.47		**Predicted R^2**	0.8576		
			Adeq Precision	29.1897		

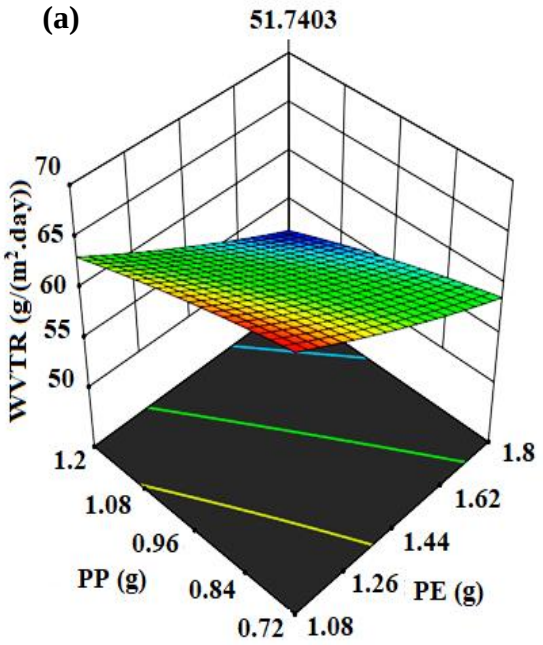
(a)
51.7403
WVTR (g/(m².day))
70
65
60
55
50
1.2
1.08
0.96
0.84
0.72
PP (g)
1.08
1.26
1.44
1.62
1.8
PE (g)

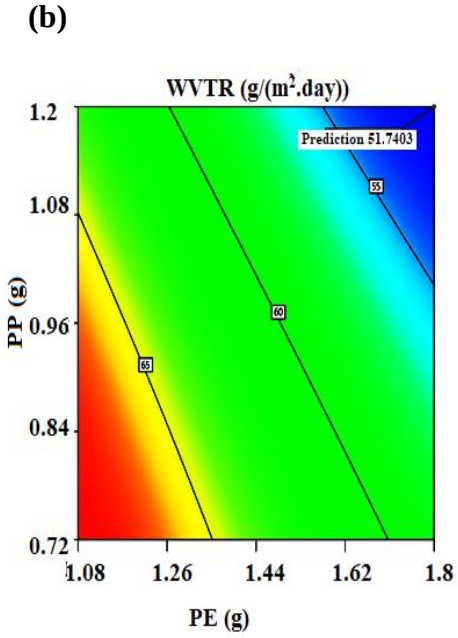
(b)
WVTR (g/(m².day))
Prediction 51.7403
55
60
65
1.2
1.08
0.96
0.84
0.72
PP (g)
1.08
1.26
1.44
1.62
1.8
PE (g)

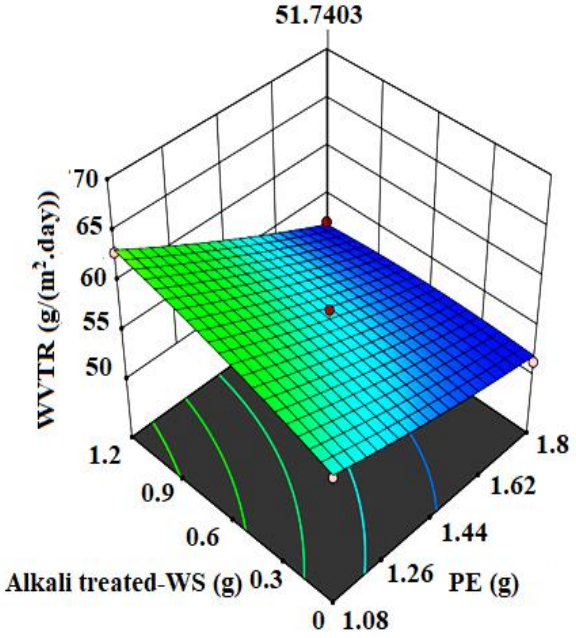
51.7403
WVTR (g/(m².day))
70
65
60
55
50
1.2
0.9
0.6
0.3
0
Alkali treated-WS (g)
1.08
1.26
1.44
1.62
1.8
PE (g)

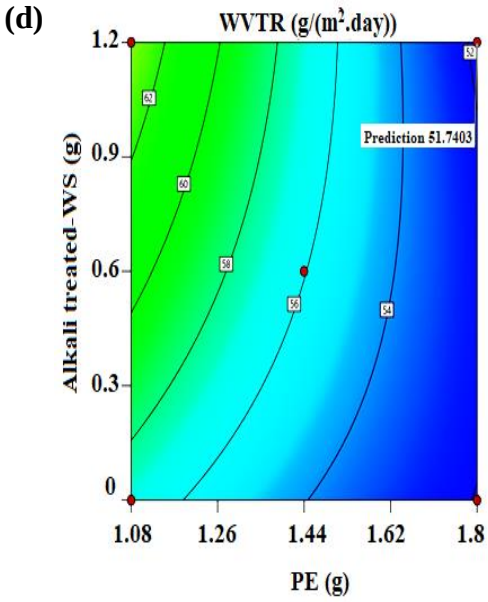
(d)
WVTR (g/(m².day))
Prediction 51.7403
52
54
56
58
60
62
1.2
0.9
0.6
0.3
0
Alkali treated-WS (g)
1.08
1.26
1.44
1.62
1.8
PE (g)

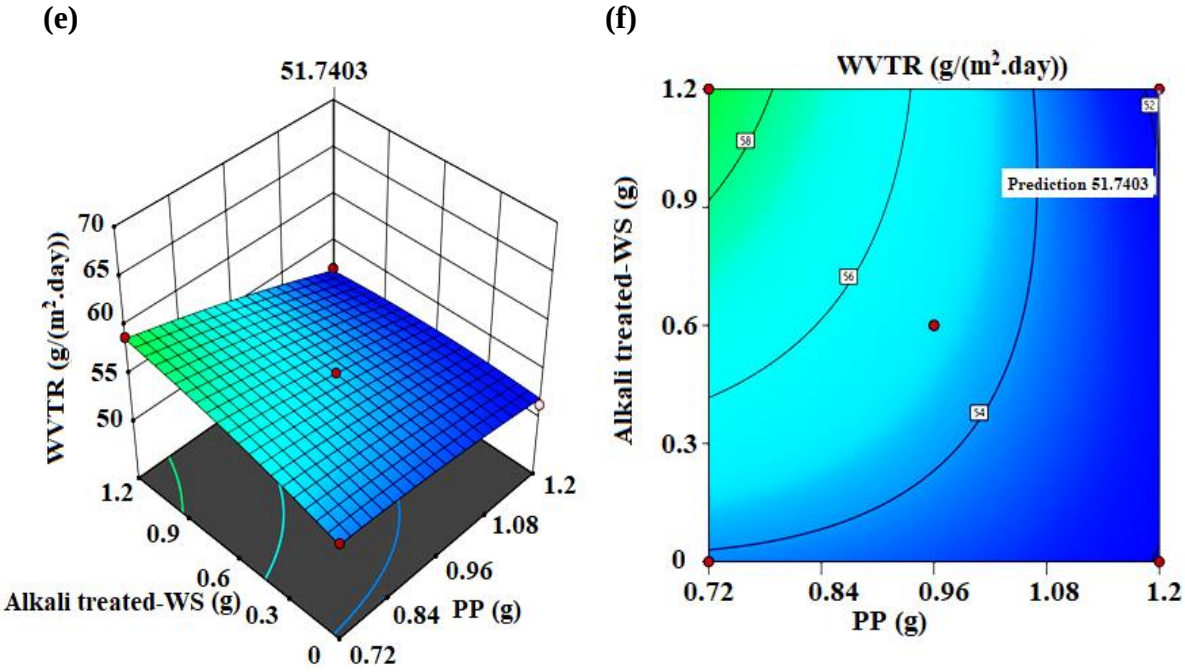

Figure 3.8 Three-dimensional response surface and contour plots of water vapor transmission rate showing the effect of (a) and (b) polypropylene and polyethylene; (c) and (d) alkali treated-WS and polyethylene; (e) and (f) alkali treated-WS and polypropylene.

3.3.3 Optimization of the statistical model

The optimization run was performed with 42.93 wt. % of polyethylene, 28.62 wt.% of polypropylene and 28.43 wt.% of alkali treated-WS. Predicted responses at optimum parameters provided by RSM are 45.018 MPa for tensile strength, 120% for elongation at break and 51.740 g m^{-2} day^{-1} for water vapor transmission rate. The RSM study shows that the desirable properties could be obtained with optimized conditions. The experimental results with the optimized parameters yield 45.010 MPa for tensile strength, 119.98 for elongation at break (%) and 51.890 for water vapor transmission rate. The error in all results is found to be very less. This small error in results exhibits the reliable response obtained using CCD process optimization technique.

3.3.4 Characterization of the optimized polyethylene/polypropylene/alkali treated-wheat straw bio-composite film

The synthesized PE/PP, PE/PP/Native-wheat straw and PE/PP/Alkali treated- wheat straw composite films were characterized using SEM, XRD, mechanical testing, contact angle, WVTR and Optical characteristics test.

3.3.4.1 SEM analysis

In order to elucidate the surface morphology of PE/PP, PE/PP/Native-wheat straw and PE/PP/Alkali treated- wheat straw composite films, SEM analysis was performed. 10x magnification SEM images have been depicted to examine the adhesion of polymer and treated-biomass. Figure 3.9(a) exhibits the plain surface of PE/PP based composite. Fractured SEM image of PE/PP/Native-wheat straw composite film is observed in Figure 3.9(b). The uniform distribution of alkali treated-WS in the matrix is observed in Figure 3.9(c).

The surface behaviour of treated-WS based polymer composites revealed the existence of strong biomass-polymer matrix adhesion. In addition, treated-WS is strongly encapsulated in PE/PP matrix which restricts the penetration by problematic ingredients. Sabetzadeh et al., 2016 used nano clay for reinforcement of polyethylene/starch-based film and observed the same results as discussed earlier. The strong adhesion was correlated with the higher mechanical strength which is confirmed in mechanical testing of the film as reported in Table 3.7.

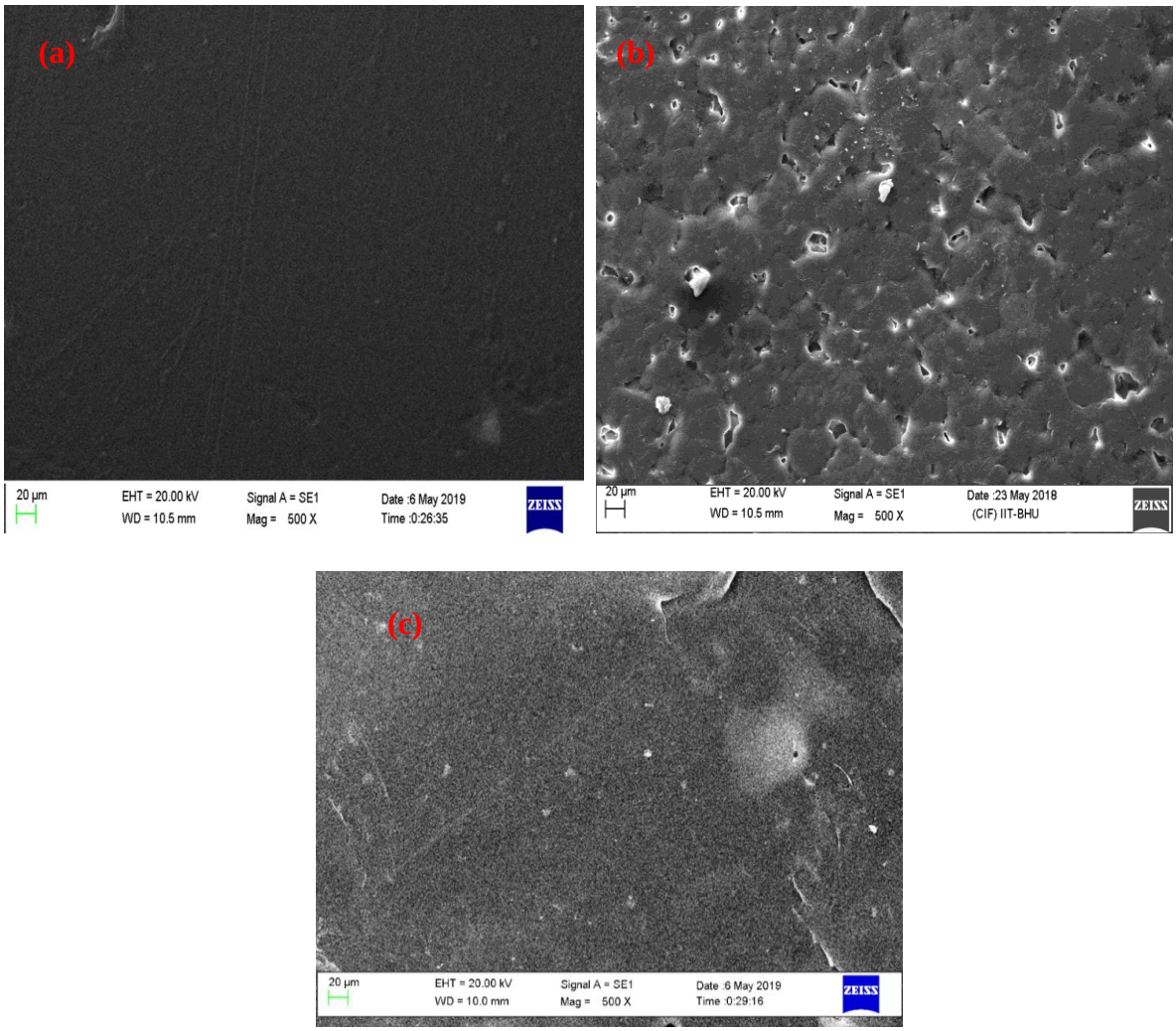

Figure 3.9 SEM analyses for all polymeric composite films (a) PE/PP film (b) PE/PP/native-WS (c) PE/PP/ alkali treated-WS composite films.

3.3.4.2 FTIR analysis

Fourier Transform Infrared spectroscopy (FTIR) is a very imperative characterization technique that detects various functional groups present in film. A particular range of wavelengths absorbed in the infrared region by film shows the existence of the specific functional group in the material. The films absorbance at different wavelengths in infrared region provides the collective information of specimen's composition and structure. In order to elucidate the chemical composition of film, the polymeric film is scanned over the wavelength region of 3500-600 cm^{-1}. FTIR spectra for PE/PP, PE/PP/native-WS and PE/PP/alkali treated-WS are shown in Figure 3.10. Peak at 770-730 cm^{-1} assigned to C-H out of the plane exhibits phenyl ring as substitution bands present in the film. Peak at 1320-1000 cm^{-1} certified C-O stretching, peak at 1385-1375 cm^{-1} and peak at 1470-1450 cm^{-1} exhibit alkanes present in the film. CH_2 stretching at 3000-2850 cm^{-1}indicates the presence of aliphatic compounds in the film. The collective information is assuring that the film is a mixture of polyethylene and polypropylene (Gulmine et al., 2002). Peaks at 1375-1300 cm^{-1} assigned to C-H wagging, 3000-2850 cm^{-1} corresponds to CH_2 stretching and 1765-1715 cm-1 assigned to C=O stretching exhibit the existence of agro-waste in the film (Yang et al., 2007).

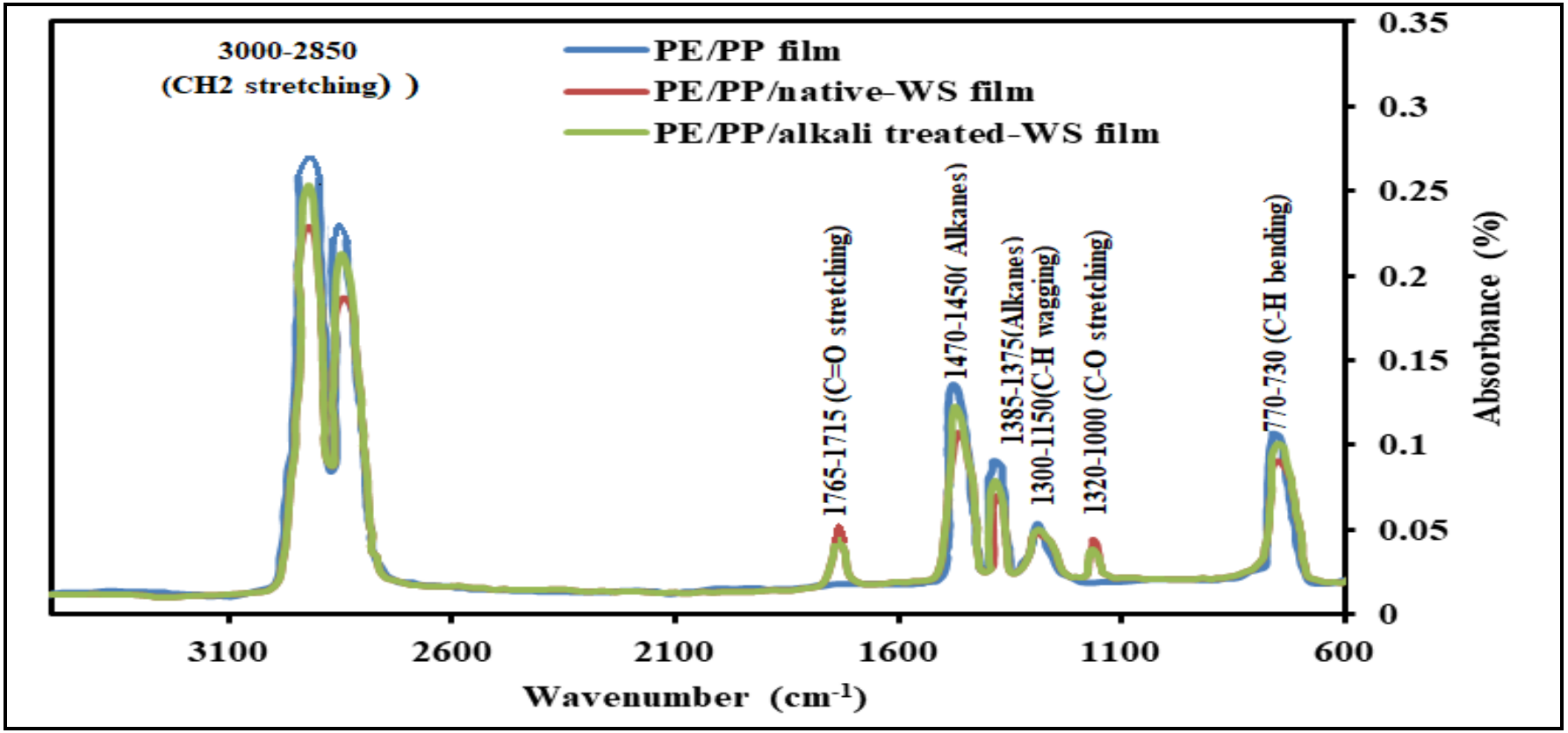

Figure 3.10 FTIR analyses for all polymeric composite films (a) PE/PP film (b) PE/PP/native-WS (c) PE/PP/ alkali treated-WS composite films.

3.3.4.3 XRD analysis

The crystalline changes in PE/PP, PE/PP/Native-wheat straw and PE/PP/Alkali treated-wheat straw composite films were analysed by using XRD analysis and are shown in Figure 3.11. There are five principle peaks observed for PE/PP, PE/PP/Native-wheat straw and PE/PP/Alkali treated- wheat straw composite films which are around 13˚, 16˚, 18˚, 21˚ and 23˚ respectively. The peak at 21.5˚ for PE/PP, 21.35 ˚ for PE/PP/Native-wheat straw and 21.48 ˚ for Alkali treated-WS are of higher intensity in XRD spectrum.

Comparable peak height at around 21˚ for both composite films is showing the increase of cellulose crystallinity in the polymer matrix. Islam et al., 2011 described that the increase in cellulose crystallinity was correlated with the decrement in the amorphous region after pre-treatment. So probably, the use of alkali treated-WS for blending with polymer matrix was maintaining the hydrophobicity of polymer matrix film which is confirmed in the contact angle measurement test of the film. Same results were reported by Kalia and Vashistha, 2012 in previous studies.

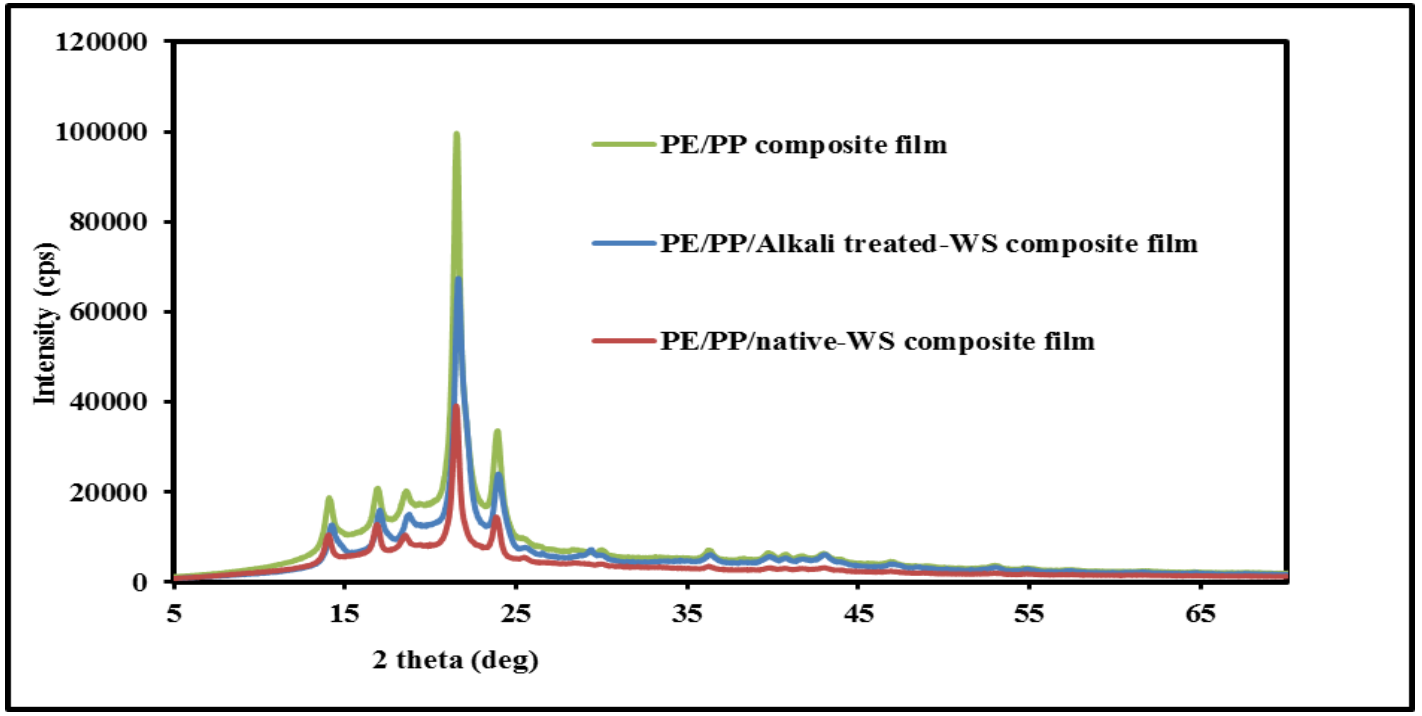

Figure 3.11 XRD analyses for all polymeric composite films (a) PE/PP film (b) PE/PP/native-WS (c) PE/PP/ alkali treated-WS composite films.

3.3.4.4 TGA analysis

TGA helps to elucidate the thermal stability of a composite film. The TGA results for PE/PP, real packaging, PE/PP/native-WS and PE/PP/Alkali treated-WS films are depicted in Figure 3.12. A small weight loss of PE/PP/native-WS is observed at 150-236 ^{O}C. Small weight loss signifies the removal of moisture and impurities from the film (El Achaby et al., 2017). TGA graphs also show that the main degradation starts around 236 ^{O}C for PE/PP/native-WS film with 3.5% weight loss, 297 ^{O}C for PE/PP/Alkali treated-WS with 2% weight loss, 332 ^{O}C for real packaging film with 3% weight loss and 342 ^{O}C for PE/PP film with 2% weight loss. Moreover, degradation ended at around 420 ^{O}C for PE/PP/native-WS film with 30% weight loss, 437^{O}C for PE/PP/alkali treated-WS film with 27% weight loss, 425^{O}C for real packaging film with 20% weight loss and 433^{O}C for PE/PP film with 19% weight loss which signify the degradation of the polymer composite chain. Another degradation ends at 469 ^{O}C for PE/PP/native-WS film with 80% weight loss, 461^{O}C for PE/PP/native-WS film with 85 % weight loss, 509 ^{O}C for real packaging film with 89% weight loss and 490^{O}C for PE/PP film with 88 % weight loss in thermal degradation graph.

Seggiani et al., 2017, reported the decrement in thermal stability of lignocellulosic biomass based composite film. It can be concluded that there may be de-bonding between the PP/PE and Native-WS (Maity et al., 2012). The addition of alkali treated–WS has a remarkable impact on the thermal stability of PP/PE based composite film. The degradation temperature shifts towards higher temperatures as polymer matrix interacted with treated-agro-waste. Treated-WS restricts the thermal degradation of polymer chain which is similar to the results reported by Perumal et al., 2018. The thermal stability of PE/PP/Alkali treated-WS film is found higher in a TGA thermo-gram which is comparable with the PE/PP and real packaging film. This represents that

of hemicellulose and lignin present in wheat straw were removed as a result of chemical treatment and its outcome is better interfacial interaction between the polymer matrix and treated wheat straw. Similar results have been reported by Chang et al., 2010 in their research article.

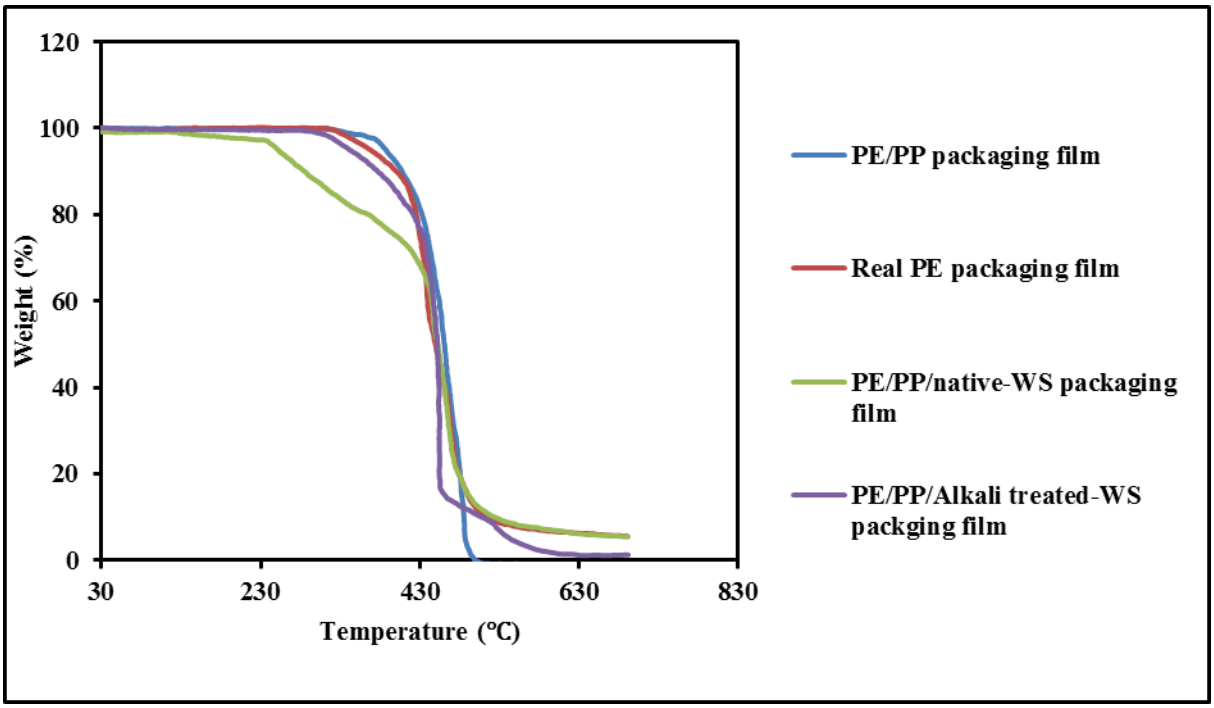

Figure 3.12 TGA analyses for all polymeric composite films (a) PE/PP film (b) Real packaging (c) PE/PP/native-WS (d) PE/PP/ alkali treated-WS composite films.

3.3.4.5 Mechanical testing

In this test, the mechanical stability of PE/PP, real polyethylene packaging, real polyester packaging, PE/PP/Native-wheat straw and PE/PP/Alkali treated- wheat straw composite films have been investigated (Figure 3.13). Tensile strength and flexibility tests for all films have been summarized in Table 3.7. The tensile strength of PE/PP, real PE packaging, real polyester packaging, PE/PP/Native-wheat straw and PE/PP/Alkali treated- wheat straw composite films are 46.5 MPa, 29.07 MPa, 25.50 MPa, 34 MPa, and 45.010 MPa, respectively. On the other hand, the elongation limit of PE/PP, real PE packaging, real polyester packaging, PE/PP/Native-wheat straw and PE/PP/Alkali treated- wheat straw composite films are 122.05%, 124.92%, 117.37 %, 116.20% and 119.98%, respectively.

A notable decrement in tensile strength is observed for polymer incorporated with native-wheat straw. Moreover, it also signified a poor adhesion between polymer and native-wheat straw. An increase in tensile strength from 34 MPa to 45.010 MPa was observed in polymer blended with alkali treated-wheat straw which is similar to the results published by Nyambo et al., 2011 in their research article. This positive enhancement in tensile strength reveals reliability of treated-biomass based packaging film in terms of mechanical stability as compared to real PE or jute packaging films.

A clear decrease in flexible limit was observed in polymer incorporated with untreated-wheat straw biomass. Sánchez-Safont et al., 2018 prepared different lignocellulosic waste-based packaging film and reported similar results in their article. Moreover, the elongation limit increased from 116.20% to 119.98 % after blending of treated-wheat straw with the polymer matrix. The flexible limit is improved by enhancing the

suitability of fiber in the polymer matrix using alkali treatment and renders it comparable with real packaging or PE/PP films.

There is a remarkable improvement in mechanical stability after incorporating treated-wheat straw with the polymer matrix. Hence, it can be stated that polymer incorporated with treated-wheat straw exhibits the suitability of polymeric composite films in packaging applications.

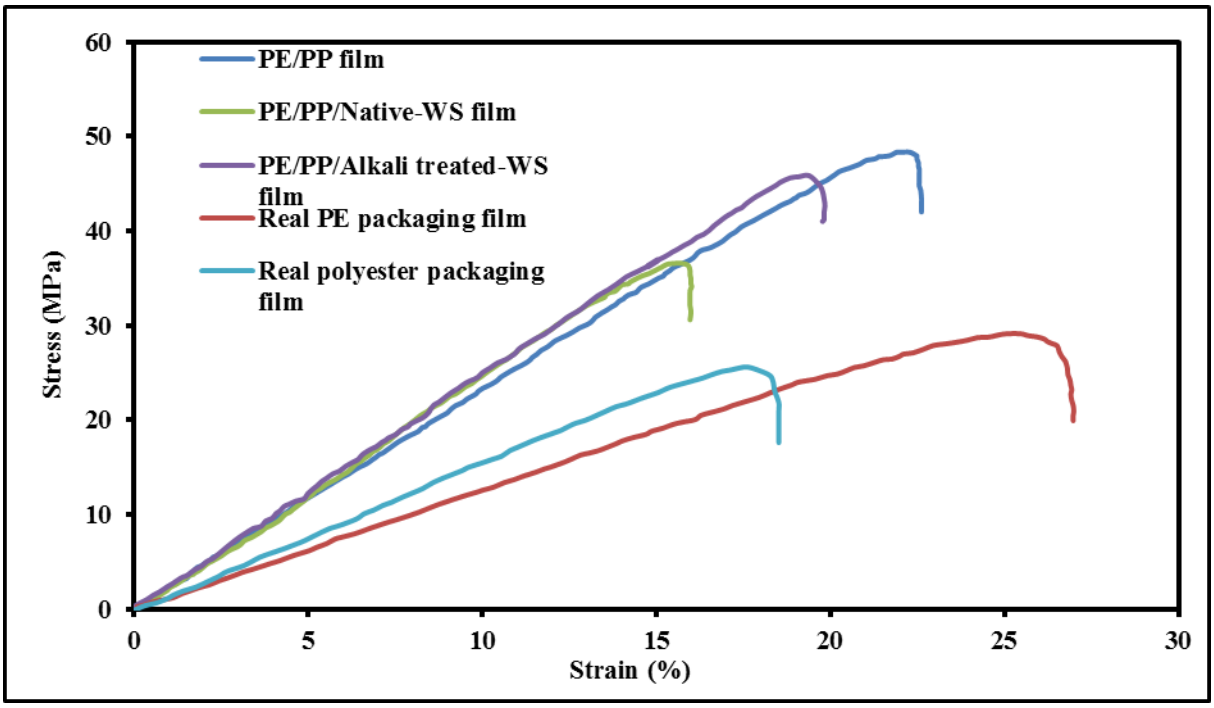

Figure 3.13 Stress vs. strain curve for polymeric composite films (a) PE/PP film (b) Real PE packaging (c) Real polyester packaging (d) PE/PP/native-WS (e) PE/PP/ alkali treated-WS composite films.

Table 3.7 Tensile stress, Yield strength, Elongation at break and Young modulus for all polymeric composite films.

Film	Tensile stress at break (MPa)	Yield strength (MPa)	Elongation at break (%)	Young Modulus (MPa)
PE(60 wt.%)/PP (40 wt.%)	46.5	45.34	122.05	210.88
Real PE packaging	29.07	28.45	124.92	116.65
Real polyester packaging	25.50	25.14	117.37	146.80
PE (42.93 wt.%)/ PP (28.62 wt.%)/ native-WS (28.43 wt.%)	34	33.15	116.20	209.87
PE (42.93 wt.%)/ PP (28.62 wt.%)/ Alkali treated-WS(28.43 wt.%)	45.010	44.19	119.98	225.27

3.3.3.6 Contact angle

Water-repelling behaviour of polymeric composite films was investigated using contact angle test. Contact angle values for PE/PP, real polyethylene packaging, real polyester packaging, PE/PP/Native-wheat straw and PE/PP/Alkali treated- wheat straw composite films are depicted in Table 3.8.

The contact angle values for PE/PP, real polyethylene packaging, real polyester packaging, PE/PP/Native-wheat straw and PE/PP/Alkali treated- wheat straw composite films are 121°, 120°, 60°, 92° and 117°, respectively. The contact angle value for both biomasses based polymeric composite films is greater than 90°and higher as compared to real polyester packaging film. It can be attributed to the existence of weak surface

energy between film and liquid as compared to surface tension of the water. This test outcome suggested the use of alkali treated-WS in a polymer matrix for green reinforcement packaging applications (Baek et al., 2012; Tang et al., 2009).

3.3.3.7 WVP test

Water vapor transmission rate and water vapor permeability provides the idea about the permeating water through the film at certain specified conditions such as temperature, time, saturation pressure and relative humidity. WVP and WVTR are reliable techniques for measuring the permeability for vapor barrier. These tests are very crucial for selecting a valuable film for water resistant and food packaging applications. In this test, water vapor barrier properties for composite films were estimated and the values are depicted in Table 3.8. WVTR for PE/PP, real polyethylene packaging, real polyester packaging, PE/PP/Native-wheat straw and PE/PP/Alkali treated- wheat straw composite films are 47.50, 45.1, 268.86, 132.10 and 51.890 $g.m^{-2}.day^{-1}$, respectively. Moreover, WVP for PE/PP, real polyethylene packaging, real polyester packaging, PE/PP/Native-wheat straw and PE/PP/Alkali treated- wheat straw are 2.50E-11, 2.37E-11, 3.13E-10, 6.99E-11 and 2.73E-11 $g.m^{-1}. Pa^{-1}.s^{-1}$, respectively.

WVP and WVTR for PE/PP/Native-WS composite film are high due to the unsuitable blending of biomass in a polymer matrix which was confirmed in SEM analysis. It has better water affinity as compared to other polymeric composite films. Sánchez-Safont et al., 2018 and Tănase et al., 2015 have reported similar results in their research articles. After the dispersion of alkali treated-wheat straw in the polymer matrix in place of native-wheat straw, WVP and WVTR are decreased due to the roughness of composite film, which is showing better compatibility of treated biomass in polymer matrix. WVP and WVTR values for treated-WS based polymeric film are comparable

with real PE packaging and PE/PP film, and higher as compared to real polyester packaging film. As an outcome, it can be concluded that the PE/PP/Alkali treated-wheat straw has become a better substitute for polymer composite or real packaging film for packaging applications.

3.3.3.8 Dart Impact test

Impact strength is a very important parameter for evaluating the load bearing characteristics of packaging film. Impact strength has generally expressed the ability of a material to resist a sudden load applied on the surface of the film. Dart impact tester is a technical way to calculate the impact energy and force essential to fracture the surface of film. In this test, a dart of known weight is dropped perpendicular from a height of 43 cm to the surface of the polymeric film in order to calculate the impact strength of the material until it partially or completely breaks the film.

Dart impact energy, dart impact strength, striking velocity before impact and dart failure weight for PE/PP, real polyethylene packaging, real polyester packaging, PE/PP/native-WS and PE/PP/alkali treated-WS film is shown in Table 3.8. The impact strength for PE/PP, real packaging, PE/PP/native-WS and PE/PP/alkali treated-WS film is 2069.10 J/m, 2052 J/m, 1453 J/m, 1573.2 J/m, and 2000.7 J/m respectively. The impact strength of PE/PP is found higher as compared to real packaging films. There is a certain decrement in impact strength after incorporation of native-WS in polymeric film due to the recalcitrance nature of biomass. But after alkali treatment, impact strength increases up to 27% showing the reliability of treated-WS reinforced polymeric film for packaging applications.

3.3.3.9 Optical characteristics test

Evaluation of optical characteristics of synthesized films is necessary to consider in packaging applications. Transparency test provides the idea about the visibility of the synthesized film. It is generally expressed in percentage. In this optical characteristic test, visible light transmission rate over 400-800nm wavelength range for PE/PP, real polyethylene packaging, real polyester packaging, PE/PP/Native-WS and PE/PP/Alkali treated-WS films were examined the results and have been compiled in Table 3.8**.** The optical transparency of native-WS based polymeric composite film is very less due to non-uniform blending of untreated-WS in the polymer matrix but higher as compared to real polyester packaging film. The transparency of alkali treated-WS reinforced polymer matrix is 18.65% at 800 nm which is higher as compared to native-WS based polymeric film. This could be due to reducing the recalcitrance nature of agro-waste after pre-treatment. But the light transmission rate for alkali treated-WS based composite film is estimated to be less as compared to the pure polymer composite and real packaging films. In addition, film still has hazing transparency due to the uniform distribution of wheat straw in the polymer matrix. Similar results were reported by Zeng et al., 2005 and Liu et al., 2014 in their previous published studies. Thus, PE/PP/Alkali treated-WS green composite with haze transparency could be used for packaging applications.

Table 3.8 Contact angle, Dart impact velocity, Dart impact failure weight, WVTR, WVP and light transmission rate for all polymeric composite films.

Film	**Contact angle (deg)**	**Dart Impact velocity before strike (m/s)**	**Dart Impact Failure weight (g)**	**Dart Impact strength (J/m)**	**WVTR ($g\ m^{-2}\ day^{-1}$)**	**WVP ($g.m^{-1}.Pa^{-1}.s^{-1}$)**	**Light transmission rate through a different visible wavelength range (nm)**		
							400	**600**	**800**
PE/PP	121^{o}±4	2.93	121	2069.10	47.50	2.50E-11	30.5±0.02	34.30±0.01	41.20±0.02
Real packaging	120^{o}±1	2.93	120	2052	45.1	2.37E-11	90±0.015	92±0.02	95±0.01
Real polyester packaging	60±4	2.93	85	1453	268.86	3.13E-10	1.76±0.08	1.90±0.06	1.96±0.05
PE/PP/native-WS	92^{o}±2	2.93	92	1573.2	132.10	6.99E-11	5.5± 0.02	7.70±0.04	8.2±0.03
PE/PP/Alkali treated-WS	117^{o}±5	2.93	117	2000.7	51.890	2.73E-11	10.25±0.05	15.4±0.04	18..65±0.07

3.4 Conclusions

The response surface methodology for PE/PP/Alkali treated-WS biocomposite film was successfully applied with 0.996 selectivity. The optimum concentrations for polyethylene, polypropylene and wheat straw were 1.8g (42.93 wt.%), 1.2g (28.62 wt.%) and 1.192 g (28.43 wt.%), respectively. The optimized results for tensile strength, elongation at break (%) and water vapor migration rate using independent variables for biocomposite film were 45.018 MPa, 120% and 51.740 $g.m^{-2}.day^{-1}$, respectively. The optimum results predicted by RSM were equable with the experimental results. However, the equable results were showing the accuracy of CCD-RSM model. In addition, the optimized film was also characterized using SEM, XRD, mechanical testing, contact angle and optical characteristics test. SEM and XRD analysis showed a roughened surface of treated-WS in the polymer matrix. TGA analysis and Contact angle test explored the higher melting point of film with benchmark water repelling property. Optical characteristics explained the hazing transparency of film. The properties of alkali treated-WS based polymeric film is comparable with PE/PP or real polyethylene packaging film. So, it can be concluded that these outcomes can be associated with the use of treated-WS for better mechanical strength, lower water migration rate with moderate elongation for promising green packaging applications.